



# The Cytochrome $b_6f$ Complex Is Not Involved in Cyanobacterial State Transitions<sup>[OPEN]</sup>

Pablo I. Calzadilla,<sup>a,1</sup> Jiao Zhan,<sup>a,b,1</sup> Pierre Sétif,<sup>a</sup> Claire Lemaire,<sup>a</sup> Daniel Solymosi,<sup>c</sup> Natalia Battchikova,<sup>c</sup> Qiang Wang,<sup>b,d</sup> and Diana Kirilovsky<sup>a,2</sup>

<sup>a</sup>Institute for Integrative Biology of the Cell (I2BC), Commissariat à l'énergie atomique et aux énergies alternatives, Centre national de la recherche scientifique, Université Paris-Sud, Université Paris-Saclay, 91198 Gif sur Yvette, France

<sup>b</sup>Key Laboratory of Algal Biology, Institute of Hydrobiology, Chinese Academy of Sciences, Wuhan 430072, Hubei, China

<sup>c</sup>Molecular Plant Biology Lab, Biochemistry Department, Faculty of Science and Engineering, University of Turku, Turku, FI-20014, Finland

<sup>d</sup>Key Laboratory of Plant Stress Biology, State Key Laboratory of Cotton Biology, School of Life Sciences, Henan University, Kaifeng 475004, China

ORCID IDs: 0000-0003-2941-6037 (P.I.C.); 0000-0003-2860-7632 (J.Z.); 0000-0002-6101-4006 (P.S.); 0000-0002-0789-5121 (C.L.); 0000-0003-3655-3654 (D.S.); 0000-0001-5176-3639 (N.B.); 0000-0002-7388-4703 (Q.W.); 0000-0003-2146-3103 (D.K.)

**Photosynthetic organisms must sense and respond to fluctuating environmental conditions in order to perform efficient photosynthesis and to avoid the formation of dangerous reactive oxygen species. The excitation energy arriving at each photosystem permanently changes due to variations in the intensity and spectral properties of the absorbed light. Cyanobacteria, like plants and algae, have developed a mechanism, named “state transitions,” that balances photosystem activities. Here, we characterize the role of the cytochrome  $b_6f$  complex and phosphorylation reactions in cyanobacterial state transitions using *Synechococcus elongatus* PCC 7942 and *Synechocystis* PCC 6803 as model organisms. First, large photosystem II (PSII) fluorescence quenching was observed in State II, a result that does not appear to be related to energy transfer from PSII to PSI (spillover). This membrane-associated process was inhibited by betaine, Suc, and high concentrations of phosphate. Then, using different chemicals affecting the plastoquinone pool redox state and cytochrome  $b_6f$  activity, we demonstrate that this complex is not involved in state transitions in *S. elongatus* or *Synechocystis* PCC6803. Finally, by constructing and characterizing 21 protein kinase and phosphatase mutants and using chemical inhibitors, we demonstrate that phosphorylation reactions are not essential for cyanobacterial state transitions. Thus, signal transduction is completely different in cyanobacterial and plant (green alga) state transitions.**

## INTRODUCTION

Photosynthetic organisms must cope with changes in the quality and quantity of incoming light. In order to survive and to optimize the use of light, they must adapt to changing environmental conditions by regulating the energy arriving at their reaction centers. Specific illumination of photosystem II (PSII) or photosystem I (PSI) creates an energy imbalance that leads to the over-reduction or over-oxidation of the intersystem electron transport chain. Murata (1969) and Bonaventura and Myers (1969) were the first to propose a mechanism, called “state transitions,” which rebalances the activity of reaction centers I and II. Two states were defined: State I, induced by light preferentially absorbed by PSI and characterized by a high PSII to PSI fluorescence ratio; State II, induced by light preferentially absorbed by PSII and characterized by a low PSII to PSI fluorescence ratio. The transition from one state to the other is triggered by changes in the redox state of the

plastoquinone (PQ) pool (Allen et al., 1981; Mullineaux and Allen, 1990); oxidation of the PQ pool induces the transition to State I and its reduction induces the transition to State II.

In plants and green algae, reduction of the PQ pool induces the activation of a specific kinase that phosphorylates the membrane-bound light-harvesting complex II (LHCII). The phosphorylated LHCII detaches from PSII and attaches to PSI during the transition from State I to State II. Oxidation of the PQ pool deactivates the kinase and a phosphatase dephosphorylates LHCII, which again migrates to PSII. The migration of LHCII from one photosystem to the other allows for a readjustment in the distribution of excitation energy arriving at PSI and PSII (see review in Minagawa, 2011).

In red algae and cyanobacteria, the principal PSII antenna is the phycobilisome (PBS), a large extramembrane complex constituted by phycobiliproteins organized in a core from which rods radiate (reviews can be found in Glazer, 1984; MacColl, 1998; and Adir, 2008). As a consequence, the processes involved in state transitions in these organisms differ. In red algae, the large fluorescence quenching induced by the illumination of dark-adapted cells is related to two different mechanisms: a PSII non-photochemical-quenching mechanism induced by a low luminal pH (Delphin et al., 1995, 1996; Kowalczyk et al., 2013; Krupnik et al., 2013), in which the fluorescence quenching occurs at the level of the reaction centers (Krupnik et al., 2013); and state transitions induced by changes in the redox state of the PQ pool, which

<sup>1</sup> These authors contributed equally to this work.

<sup>2</sup> Address correspondence to diana.kirilovsky@cea.fr.

The author responsible for distribution of materials integral to the findings presented in this article in accordance with the policy described in the Instructions for Authors (www.plantcell.org) is: Diana Kirilovsky (diana.kirilovsky@cea.fr).

<sup>[OPEN]</sup>Articles can be viewed without a subscription.

www.plantcell.org/cgi/doi/10.1105/tpc.18.00916

## IN A NUTSHELL

**Background:** Plants, algae, and cyanobacteria harvest solar energy and convert it into chemical energy through photosynthesis. The photosynthetic apparatus involves two pigment protein complexes (the photosystems: PSII and PSI), which capture solar light and perform photochemical reactions, and a third complex (cytochrome *b<sub>6</sub>f*), which participates in electron transport between the photosystems. Photosystem activities must be balanced under fluctuating environmental conditions. This balance is achieved by a mechanism called state transitions, which is regulated by the redox state of the plastoquinone (PQ) pool, a membrane-soluble electron carrier between PSII and cytochrome *b<sub>6</sub>f*. In plants and green algae, the redox sensor of the PQ pool is cytochrome *b<sub>6</sub>f*, which interacts with a specific kinase of the major membrane chlorophyll antenna known as Light Harvesting Complex II. The molecular mechanism of cyanobacterial state transitions and its transduction signal are still a matter of discussion, although many hypotheses have been proposed.

**Question:** We aimed to revisit cyanobacterial state transitions, focusing on the signal transduction pathway and the membrane changes involved in its mechanism.

**Findings:** The PQ pool redox state also regulates cyanobacterial state transitions. However, using *Synechocystis* PCC 6803 and *Synechococcus elongatus* as model organisms, we clearly demonstrate that cytochrome *b<sub>6</sub>f* is neither the sensor nor the signal transducer in this process. In addition, construction and characterization of kinase and phosphatase *Synechocystis* mutants allowed us to show that there is no specific phosphorylation reaction that participates in cyanobacterial state transitions. These results were confirmed using kinase and phosphatase inhibitors. Thus, the signal transduction pathways involved in state transitions in cyanobacteria and plants (green algae) are completely different. Finally, we provide evidence suggesting that membrane changes at the level of PSII play an important role in cyanobacterial state transitions.

**Next steps:** Our results provide the basis for a new research hypothesis in cyanobacterial state transitions. The next step will be to identify the PQ pool sensor and the types of changes that occur at the level of PSII.

involve changes in energy transfer from PSII to PSI (spillover; Ley and Butler, 1980; Kowalczyk et al., 2013). The relative importance of each mechanism varies among strains (Delphin et al., 1996; Kowalczyk et al., 2013). In cyanobacteria, the molecular mechanism of the PQ-pool dependent state transitions remains largely obscure. This process, which involves fluorescence changes occurring upon illumination of dark-adapted cells or under illumination with light absorbed more specifically by PSII or PSI, indeed remains an open question, despite the many studies resulting in the proposal of several hypotheses and models.

In the mobile-PBS model, the movement of PBSs induces changes in direct energy transfer from PBS to PSII and PSI (Allen et al., 1985; Mullineaux and Allen, 1990; Mullineaux et al., 1997). This model attributes the low PSII fluorescence yield in State II to a lower amount of energy transfer from PBSs to PSII, together with larger energy transfer to PSI. The observations that PBSs are able to rapidly move on the thylakoid surface (Mullineaux et al., 1997) and that chemicals inhibiting PBS diffusion also inhibit state transitions support this model (Joshua and Mullineaux, 2004; Li et al., 2004, 2006). In the spillover model, the energy transfer from PBS to PSII remains equal in both states, but the excess energy absorbed by PSII is transferred to PSI (spillover) in State II via a process involving the movement of photosystems (Ley and Butler, 1980; Bruce and Biggins, 1985; Olive et al., 1986; Biggins and Bruce, 1989; Biggins et al., 1989; Vernotte et al., 1992; El Bissati et al., 2000; Federman et al., 2000). The hypothesis that changes at the level of photosystems are responsible for state transitions is supported by various observations: state transitions occur in mutants lacking PBSs (Bruce et al., 1989; Olive et al., 1997; El Bissati et al., 2000); state transitions are accompanied by structural changes in membranes (Vernotte et al., 1992; Folea et al., 2008) and PSI monomerization/trimerization (Kruip et al.,

1994; Schluchter et al., 1996; Aspinwall et al., 2004); and membrane fluidity influences state transitions (El Bissati et al., 2000). Nevertheless, there has been no clear demonstration that the spillover is larger in State II than in State I, although some studies have suggested this (see Mullineaux et al., 1991; Bruce and Salehian, 1992). It was also proposed that these two mechanisms coexist and are responsible for the fluorescence changes observed in state transitions: movement of PBS (changes in direct energy transfer from PBSs to photosystems) and movement of photosystems (changes in spillover; Scott et al., 2006). However, more recent studies have questioned the definition of cyanobacterial state transitions as a rebalance of excitation energy arriving to one or another photosystem. The increase in fluorescence in State I has principally been associated with the functional detachment of PBS from the photosystems (Kaňa et al., 2009; Kaňa, 2013; Chukhutsina et al., 2015), whereas the decrease in fluorescence in State II was mainly attributed to a specific fluorescence quenching of PSII not involving spillover (Ranjbar Choubeh et al., 2018).

Furthermore, the states of plants and cyanobacteria in darkness differ: while plants are generally in State I, cyanobacteria are in State II (Aoki and Katoh, 1982; Mullineaux and Allen, 1986). In cyanobacteria, respiration and photosynthesis occur in the thylakoid membranes, and PQ, cytochrome (cyt) *b<sub>6</sub>f* and plastocyanin (or cyt *c<sub>6</sub>*) are electron carriers common to both electron transport chains (see a review in Mullineaux, 2014). During respiration, the homologs of mitochondrial complex I (NDH-1) and complex II (succinate dehydrogenase, SDH) reduce the PQ pool, and different oxidases oxidize it (for a review, see Mullineaux, 2014). Different cyanobacterial strains present different PQ pool reduction states in darkness, giving different levels of dark PSII fluorescence (see, for example, Misumi et al., 2016). Upon

illumination, PSI is activated and the PQ pool becomes more oxidized, leading to State I (Mullineaux and Allen, 1990; Campbell et al., 1998).

In plants and green algae, the redox sensor of the PQ pool is the cyt  $b_6f$  complex, which interacts with a specific kinase of the major membrane chlorophyll (Chl) antenna, LHCII (Wollman and Lemaire, 1988). Phosphorylation of LHCII trimers induces their detachment from PSII and partial (or total) attachment to PSI, inducing the transition to State II (Kyle et al., 1984). Two reports suggest that cyt  $b_6f$  also plays a role in cyanobacterial state transitions (Mao et al., 2002; Huang et al., 2003). However, further evidence is still needed to confirm its direct involvement. In this sense, the relationship between phosphorylation and cyanobacterial state transitions is also an open question. Allen and coworkers suggested that specific types of phosphorylation could occur during state transitions (Allen et al., 1985), but this was not confirmed in more recent works. Nevertheless, analysis of phospho-proteomes showed that phosphorylation takes place in PBSs and photosystems (Yang et al., 2013; Chen et al., 2015; Spät et al., 2015). In addition, when residues Ser22, 49, and 154 and Thr94 of phycocyanin (PC; PBS protein) were mutated to non-phosphorylatable amino acids in *Synechocystis* cells, the kinetic and amplitude of transition to State I induced by light illumination of dark-adapted cells appeared to be affected (Chen et al., 2015). Some functions of Ser/Thr kinases (Spk) have already been described. For example, SpkA is involved in the control of cell motility (Kamei et al., 2001; Panichkin et al., 2006); SpkB participates in the oxidative stress response by phosphorylating glycyl-tRNA-synthetase  $\beta$ -subunit (Mata-Cabana et al., 2012); SpkE might be involved in the regulation of nitrogen metabolism (Galkin et al., 2003); SpkD might be involved in adjusting the pool of tricarboxylic acid cycle metabolites (Laurent et al., 2008); SpkG plays an essential role in high-salt resistance (Liang et al., 2011); SpkC, SpkF, and SpkK are involved in the phosphorylation of the GroES chaperone protein (Zorina et al., 2014); and SpkG is involved in the phosphorylation of ferredoxin 5 protein (Angeleri et al., 2018).

As a whole, the molecular mechanism behind cyanobacterial state transitions is still a matter of discussion, although many hypotheses have been proposed. Therefore, we decided to further study this mechanism by specifically addressing the role of the cyt  $b_6f$  complex in this process.

In the past decades, state transitions have mainly been studied in the cyanobacteria *Synechocystis* PCC 6803 (hereafter *Synechocystis*; for example, Vernotte et al., 1992; Emlyn-Jones et al., 1999; McConnell et al., 2002; Kondo et al., 2009; Chukhutsina et al., 2015), *Synechococcus* PCC7002 (McConnell et al., 2002; Dong and Zhao, 2008; Dong et al., 2009) and *Spirulina platensis* (Li et al., 2004, 2006). In these strains, the changes in fluorescence related to state transitions (dark versus blue [or far-red] illumination) are rather small, which makes mechanistic studies difficult. The differences in PSII fluorescence in darkness (State II) and under blue light illumination (State I) are significantly larger in *Synechococcus elongatus* strain than in *Synechocystis*. Therefore, in our study, we characterized state transitions in *S. elongatus* and compared them to those in *Synechocystis*, which allowed us to obtain clearer conclusions. Our results confirm data demonstrating that a large amplitude of PSII fluorescence quenching is induced in State II in *S. elongatus* (Ranjbar Choubeh

et al., 2018). This PSII quenching appears to be unrelated to spillover. In addition, not only do we show that the results and arguments used to link the cyt  $b_6f$  complex with state transitions were not conclusive, but we also demonstrate that cyt  $b_6f$  and protein phosphorylation reactions do not participate in this process in cyanobacteria. Thus, different signaling pathways are involved in state transitions in cyanobacteria compared with plants and green algae.

## RESULTS

### State Transitions in *S. elongatus* and *Synechocystis*

#### 77 K Fluorescence Spectra in State II and State I

The absorbance spectra indicate that, under our growth conditions, *S. elongatus* presents a higher PC (absorbance at 620 nanometers [nm]) to Chl (absorbance at 680 nm) ratio than *Synechocystis* (Figure 1). In addition, the PSI to PSII ratio [measured by ( $F_A$ ,  $F_B$ )<sup>-</sup> and Tyrosine-D+ (TyrD<sup>+</sup>) electron paramagnetic resonance (EPR) signals] was around 2:3 in *S. elongatus* and 4:5 in *Synechocystis* cells (for details, see Methods).

Figure 2 compares the low temperature (−196.15°C) 77 K fluorescence emission spectra of dark- and blue light-adapted *S. elongatus* (A, C) and *Synechocystis* (B, D) cells. At this temperature, the fluorescence of both photosystems is visible; while at room temperature, only PSII-related fluorescence is observed.

Supplemental Figures 1 and 2 show the Gaussian decomposition of these spectra, providing a visualization of different components of the spectra. When the PBSs were preferentially excited (excitation at 590 nm), we observed a large peak at 650 to 660 nm related to PC and allophycocyanin fluorescence; a peak at 683 nm related to the Chl binding protein CP43 and the last emitters of PBS; a peak (or shoulder in *S. elongatus*) at 695 nm corresponding to reaction center II and CP47; and a peak at 718 nm (*S. elongatus*) or 722 nm (*Synechocystis*) related to PSI fluorescence (Van Dorssen et al., 1987; Siefermann-Harms, 1988). The PSII-related peaks at 683 and 695 nm were higher in blue light-adapted cells (State I) than in dark-adapted cells (State II). The differences between the peaks in State I and II were larger in *S. elongatus* than in *Synechocystis*. Regarding PSI, the fluorescence was similar in dark- and light-adapted cells of both strains.

When the Chl was preferentially excited (excitation at 430 nm), the PSI emission peak (at 718 nm in *S. elongatus* and 722 nm in *Synechocystis*) was the highest in both strains. In addition, the PSII-related peaks at 685 and 695 nm were much higher in *S. elongatus* than in *Synechocystis*, corresponding to a lower PSI to PSII ratio (2:3 in *S. elongatus* versus 4:5 in *Synechocystis*). The PSI-related peaks were similar in darkness and blue light illumination. The absence of changes in PSI-related fluorescence during state transitions was confirmed by normalizing the *S. elongatus* spectra with an external dye (Rhodamine B; Figure 3). The PSII-related peaks increased upon blue light illumination in both strains. Nevertheless, the emission at 695 nm increased more than the one at 683 nm (Supplemental Figures 1 and 2).

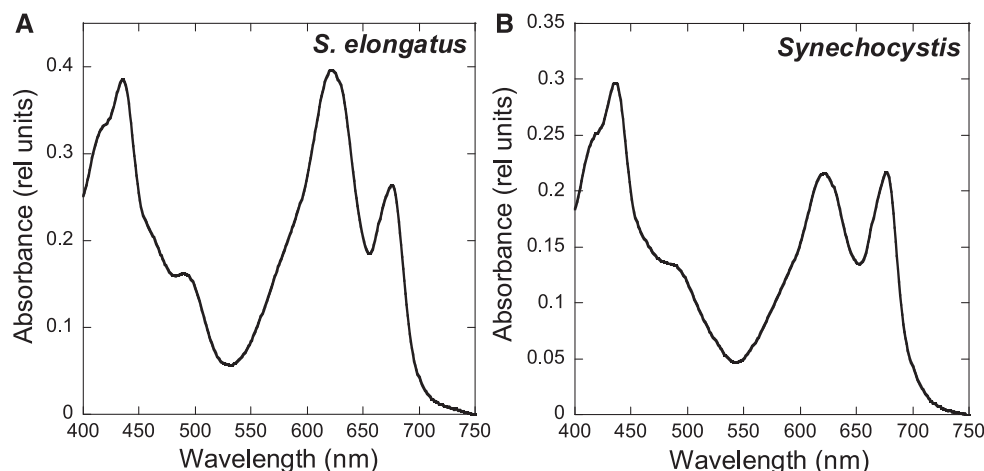


**Figure 1.** Absorption Spectra of *S. elongatus* (A) and *Synechocystis* (B) Cells.

The spectra were recorded at a Chl concentration of 2.5  $\mu\text{g}/\text{mL}$ . The curves shown are the average of three independent biological replicates (as described in Methods).

#### Effect of Hyperosmotic Buffers on State Transitions

We investigated the effects of the hyperosmotic buffers betaine (1 M, pH 7.0), Suc (1 M), and phosphate (0.5 M, pH 7.5) on state transitions in *S. elongatus* cells (Figure 4; Supplemental Figure 3). Control cells were incubated in the absence of chemicals in the dark (cells-II) or under blue light illumination (cells-I). Aliquots of these cells were rapidly frozen. Cells-II and cells-I were then incubated with chemicals for 5 min under identical conditions (dark for cells-II, blue light illumination for cells-I). Cells-II were then transferred to blue light for 5 min before freezing, whereas cells-I were transferred to dark for 5 min before freezing. We measured 77 K fluorescence spectra with excitation at 430 nm and at 590 nm. The initial effect observed upon addition of betaine and Suc was a large, general quenching of fluorescence, suggesting that these chemicals have an effect not only on PBSs but also on membranes (Figure 4; Supplemental Figure 3). The quenching effect of hyperosmotic media was previously reported in *Synechocystis* by (Papageorgiou et al., 1999), who attributed it to alterations in membrane fluidity. Nevertheless, the PBS quenching seemed to be larger than that of Chl, because the 683/695 and 660/695 ratios decreased after the addition of betaine and Suc with excitation at 590 nm. By contrast, phosphate addition had a more specific quenching effect on PBS fluorescence, as seen by the relatively large decrease in fluorescence at 660 nm (Supplemental Figure 3).

As previously observed (Joshua and Mullineaux, 2004; Li et al., 2004, 2006), no fluorescence changes were detected in 77 K emission spectra obtained by excitation at 590 nm when state transitions were tentatively induced in the presence of betaine, Suc, or phosphate (Figure 4; Supplemental Figure 3). In addition, the chemicals also inhibited the fluorescence changes observed in the 77 K emission spectra obtained with 430 nm excitation (Figure 4; Supplemental Figure 3). These results demonstrate that betaine, Suc, and phosphate also block the changes produced in the membranes. In conclusion, the effect of these hyperosmotic buffers on state transitions could be due to the inhibition of PBS movement and/or processes occurring in the membrane.

#### State Transitions Kinetics and the Redox State of the PQ Pool in Darkness

Figure 5 shows typical traces of room-temperature fluorescence kinetics measured with a pulse-amplitude-modulation (PAM) fluorometer in dark-adapted *S. elongatus* (A) and *Synechocystis* (B) cells successively illuminated by low intensities of blue and orange light. Dark-adapted cells presented a low dark maximal fluorescence ( $F_{md}$ ), indicating that the cells were in State II. Upon illumination with blue light, which preferentially excites Chl, a large and rapid increase in  $F_m'$  was observed (arriving at a maximal  $F_{mb}'$  level), indicating the transition to State I. The ratio  $F_{vb}$  to  $F_{vd}$  [variable fluorescence ( $F_v$ ) =  $F_m - F_0$ ] was  $\sim 4.0$  in *S. elongatus* but only 1.2 in *Synechocystis* cells (Figure 5). The dark  $F_{vd}/F_0$  was much smaller in *S. elongatus* than in *Synechocystis* (0.22 versus 1.09). By contrast, small differences were observed in the  $F_{vb}/F_0$  ratio (0.83 versus 1.26). These data suggest that dark-adapted *S. elongatus* cells were in a "stronger" State II than *Synechocystis* cells.

In order to elucidate whether this could be explained by a more reduced PQ pool in dark-adapted *S. elongatus*, we estimated the redox state of the PQ pool in each strain by measuring fluorescence induction curves in the absence and presence of DCMU, which inhibits electron transfer between the primary ( $Q_A$ ) and secondary ( $Q_B$ ) quinones in PSII (Figure 6). When dark-adapted cells are illuminated, the PQ pool becomes more reduced and the photochemical centers become partially closed. As a consequence, a concomitant fluorescence increase is observed until a steady state level is reached. The increased kinetics depends on both the initial redox state of the PQ pool and its rate of photochemical reduction under illumination. However, when DCMU is present, a maximum level of fluorescence is reached in which all the centers are closed and the rate of fluorescence increase depends only on the antenna size and is independent of the dark redox state of the PQ pool. Figures 7A and 7B show the fluorescence induction curves in the presence and absence of DCMU for *S. elongatus* and *Synechocystis* dark-adapted cells. The area

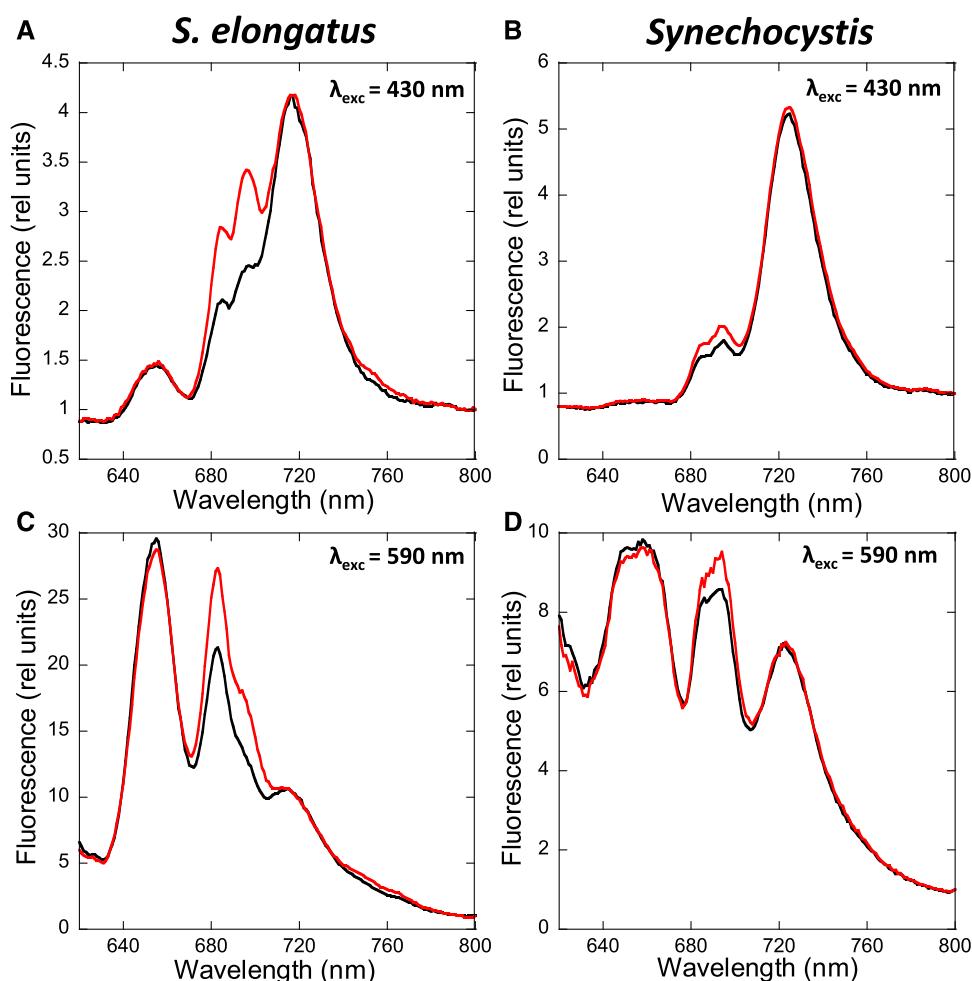


**Figure 2.** State Transitions in *S. elongatus* and *Synechocystis*.

Shown are 77 K fluorescence emission spectra of dark- (black, State II) and blue light- (red,  $85 \mu\text{M}$  photons  $\text{m}^{-2} \text{s}^{-1}$ , State I) adapted *S. elongatus* (A) and (C) and *Synechocystis* (B) and (D) cells. The excitation was done at 430 nm (A) and (B) and 590 nm (C) and (D). Normalization was done at 800 nm, and the spectra are the average of at least three independent biological replicates.

between the curves is much larger for dark-adapted *Synechocystis* than for *S. elongatus* cells (59% versus 33% of the DCMU area, respectively).

Because the area between the curves is at least partially proportional to the amount of dark-oxidized PQ (Bennoun, 1982; Srivastava et al., 1995), these results suggest that the PQ pool is more reduced in dark-adapted *S. elongatus* cells than in *Synechocystis*. However, under illumination, the rates of PQ reduction by PSII and of  $\text{PQH}_2$  (reduced PQ) reoxidation by PSI also affect the kinetics of fluorescence induction. These rates could be different between the strains, as the PSI to PSII and the phycobiliprotein to Chl ratios are different in *Synechocystis* and *S. elongatus*. Therefore, we performed a control experiment in which the PQ dark reduction level in each strain was modified without changing the size of the antenna or PSI and PSII activities. The dark PQ redox state depends on the relative activities of NDH-1/SDH and of cyanide-sensitive terminal oxidases (Cyd and Cox; Figure 6); thus, the addition of sodium cyanide (NaCN) should lead

to a large PQ-reduction level. A large effect of NaCN was observed in *Synechocystis* cells, in which the area between the curves ( $\pm$ DCMU) decreased from 59 in the absence of NaCN to 27% in its presence (Figure 7). By contrast, the effect was much smaller in *S. elongatus* cells, with only a decrease from 33 to 24% (Figure 7). These results strongly suggest that the PQ pool was more strongly reduced in *S. elongatus* than in *Synechocystis*.

The illumination of blue light-adapted cells with orange light (which preferentially excites phycobiliproteins) induced a decrease in  $F_m'$  in both cyanobacterial strains (Figure 5). In *Synechocystis* cells, the steady state  $F_{m0}$  was similar to  $F_{md}$ , whereas in *S. elongatus*, the  $F_{m0}$  was higher. As already mentioned, the “strength” of State II depends on the concentration of reduced PQ. Thus, our results indicate that the PQ pool was more strongly reduced in dark-adapted *S. elongatus* than in orange light-illuminated cells. This was not the case in *Synechocystis* cells, where the redox state of the PQ pool appeared to be similar under both conditions.



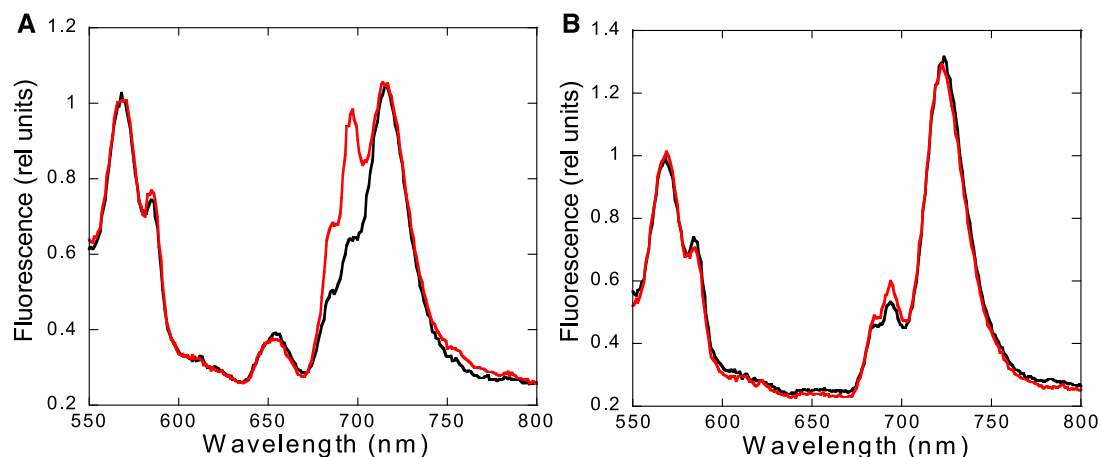


**Figure 3.** 77 K Fluorescence Emission Spectra of the Wild-Type *S. elongatus* (A) and *Synechocystis* (B) Cells Using Rhodamine B as an Internal Standard.

Cells were dark adapted for 15 min before the measurements (black lines) or incubated under blue light illumination for 5 min (red lines) before the addition of Rhodamine B (0.4  $\mu$ M). The excitation was done at 430 nm. Normalization was done at the peak of Rhodamine B at 568 nm, and the spectra are the average of at least three independent biological replicates.

### Is Cyt $b_6f$ Involved in State Transitions in *S. elongatus*?

#### Effect of DMBQ and DBMIB on State Transitions

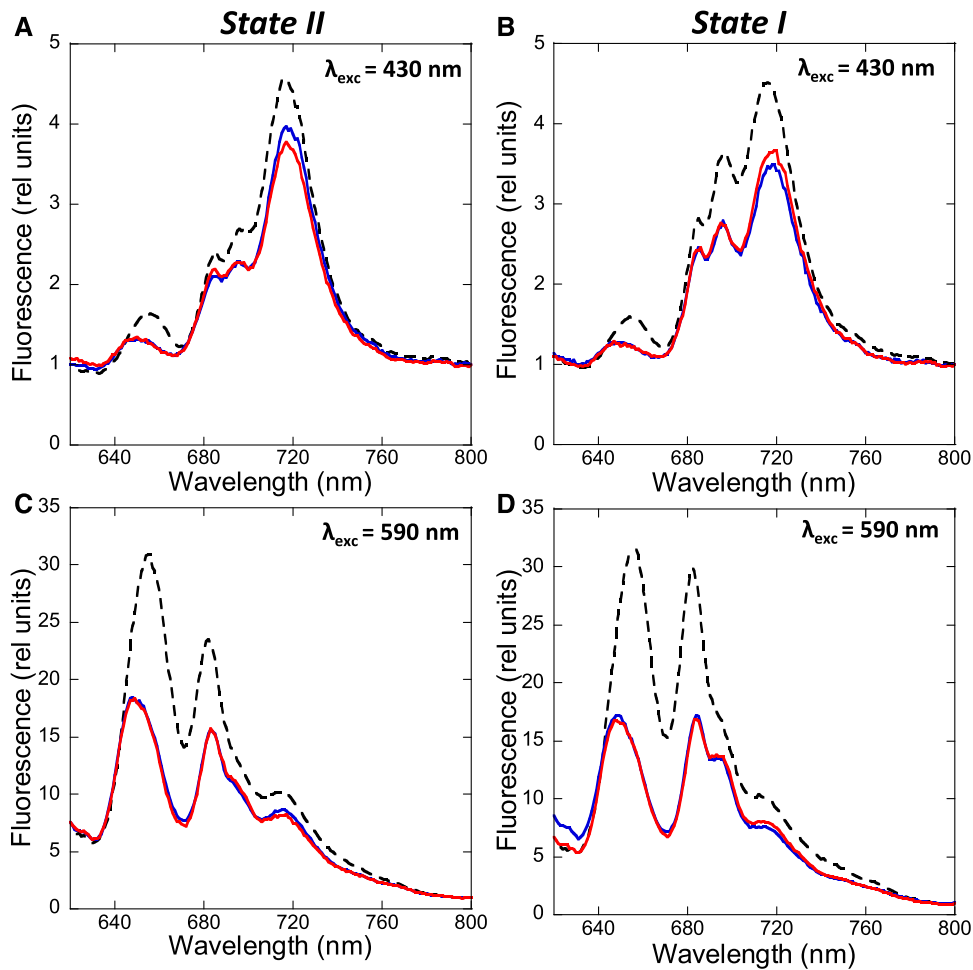
Mao et al. (Mao et al., 2002) and Huang et al. (Huang et al., 2003) proposed that cyt  $b_6f$  is involved in the signaling pathway of cyanobacterial state transitions, as observed in green algae and plants. They based their proposal on the results obtained by chemically inducing state transitions in *Synechocystis* and *Synechococcus* PCC 7002 using 2,6-dimethoxy-1,4-benzoquinone (DMBQ), p-benzoquinone (PBQ), and 2,5-dibromo-3-methyl-6-isopropyl-p-benzoquinone (DBMIB). DMBQ and PBQ accept electrons from the PQ pool (Preston and Critchley, 1988), while DBMIB inhibits cyt  $b_6f$  activity by attaching to the Qo site (the PQH<sub>2</sub> binding site), preventing reoxidation of the PQ pool (Roberts and Kramer, 2001; Figure 6). These authors found that the addition of DMBQ (or PBQ) to dark-adapted cells induced an increase in  $F_{md}$ , which they attributed to a partial transition to State I triggered by oxidation of the PQ pool. The simultaneous addition of DMBQ and DBMIB inhibited this increase. Both authors hypothesized that under these conditions, the PQ pool remained oxidized, which led them to conclude that the binding of DBMIB to the cyt  $b_6f$  Q<sub>o</sub> site was primarily involved in the transition to State II. However, none of these studies demonstrated that the PQ pool remained oxidized under these conditions.

Figure 8 shows the effect of DMBQ and DBMIB on  $F_{md}$  in dark-adapted *S. elongatus* cells. The addition of DMBQ (250  $\mu$ M) induced a slow increase in  $F_{md}$  (and  $F_0$ ) related to a partial transition to State I. Higher concentrations of DMBQ cannot be used because they induce fluorescence quenching. When DBMIB (20  $\mu$ M) was subsequently added, a rapid decrease of  $F_{md}$  (and  $F_0$ ) was observed (Figure 8A). When both chemicals were simultaneously added, the DMBQ-induced increase in fluorescence was inhibited (Figure 8B). These effects of chemicals were therefore similar to those previously observed in *Synechocystis* and *Synechococcus* PCC 7002 cells (Huang et al., 2003; Mao et al., 2003).

We then explored the dark redox state of the PQ pool in *S. elongatus* cells by analyzing the kinetics of fluorescence induction in the presence and absence of DCMU (as described in the previous section). The measurements were performed in dark-adapted cells (15 min) in the presence of DMBQ alone (250  $\mu$ M) or DMBQ and DBMIB (5 and 10  $\mu$ M). The measurements were done after 3 min of incubation with DMBQ and at 1 and 3 min after the addition of DBMIB (Figure 9). As previously mentioned, the PQ pool is reduced in dark-adapted *S. elongatus* cells: the area between the curves ( $\pm$ DCMU) is small and  $F_{md}$  is low (Figure 7A). The addition of DMBQ increased the level of  $F_{md}$  and the area between the two curves ( $\pm$ DCMU), suggesting that the PQ pool had become oxidized (Figure 9A). Because DMBQ also accepts electrons from the PQ pool during the light measurement, the larger area between the curves is also partially related to its activity during the measurement.

The addition of 5  $\mu$ M DBMIB induced a rapid decrease of  $F_{md}$  and of the area between the curves. The smaller area indicated that the PQ pool was more strongly reduced in darkness and during the light measurement in the presence of DBMIB (Figure 9B). Longer periods of incubation with DBMIB induced a larger decrease in area, indicating a larger reduction of the PQ pool even in the presence of DMBQ (Figure 9C). In line with these results, the addition of 10  $\mu$ M DBMIB had a faster and larger effect (Figures 9D and 9E). Thus, the DMBQ-induced transition to State I is inhibited by DBMIB, likely because DBMIB treatment leads to the reduction of the PQ pool, even in the presence of DMBQ, at least in *S. elongatus*.

We further studied the effects of DBMIB by adding different concentrations of this chemical (2.5, 5, 10, 15, and 20  $\mu$ M) to *S. elongatus* cells adapted to State 1 by illumination with blue-green light or by adding DMBQ in darkness (Figure 8C). Under illumination, all concentrations of DBMIB efficiently induced a large transition to State 2 with rather similar kinetics (red curves). However, concentrations higher than 5  $\mu$ M were necessary to induce the transition to State 2 in darkness and in the presence of



**Figure 4.** 77 K Fluorescence Emission Spectra of *S. elongatus* Cells Treated with Betaine.

Cells were dark adapted for 15 min (**A**) and (**C**) or incubated under blue light illumination ( $85 \text{ photons m}^{-2} \text{ s}^{-1}$ ) for 5 min (**B**) and (**D**). 77 K spectra were measured (dashed lines). Then, samples were taken after 5 min incubation with betaine (1 M) and measured (blue lines). Finally, State I (**A**) and (**C**) or State II (**B**) and (**D**) was tentatively induced by blue light illumination ( $85 \mu\text{M photons m}^{-2} \text{ s}^{-1}$ ) or darkness, respectively, for 5 min more (red lines). The excitation was done at 430 nm (**A**) and (**B**) or 590 nm (**C**) and (**D**). Normalization was done at 800 nm, and the spectra are the average of at least three independent biological replicates.

DMBQ. In this case, the rate and amplitude of the transition depended on DBMIB concentration. Thus, the same concentration of DBMIB had different effects under illumination and in darkness, in the presence of DMBQ. For example,  $5 \mu\text{M}$  DBMIB induced almost maximum fluorescence quenching under illumination but was unable to induce any quenching in darkness in the presence of DMBQ. Upon illumination of dark-adapted cells in the presence of DMBQ and different concentrations of DBMIB (2.5, 5, 10, and  $15 \mu\text{M}$ ), larger fluorescence quenching was induced (Figure 8D). These results strongly suggest that the transition to State II is induced by the reduction of the PQ pool and not by the binding of DBMIB to the  $Q_o$  site in *cyt b<sub>6</sub>f*.

#### Effect of the TMPD on State Transitions

We then looked for another chemical compound that does not interact with *cyt b<sub>6</sub>f* and can oxidize the PQ pool in the presence of

DBMIB to further confirm that this complex does not play a role in state transitions. *N, N', N'*-tetramethyl-*p*-phenylenediamine (TMPD) represents such a compound, because it restores oxygen evolution by reversing the inhibitory effect of DBMIB on the photosynthetic electron transport chain (Figure 6; Draber et al., 1970; Nanba and Katoh, 1985). Nanba and Katoh demonstrated that TMPD accepts electrons from the PQ pool and directly donates them to  $P700^+$ , bypassing the DBMIB-poisoned *cyt b<sub>6</sub>f* complex. However, TMPD is also a good electron acceptor from PSI and can generate cyclic electron transfer around PSI (Figure 6; Hiyama and Ke, 1972). This chemical has opposite effects on state transitions, depending on the preferential electron donor to TMPD (PQ pool versus PSI).

It is expected that, under blue light in the absence of DBMIB (State I), the addition of TMPD should have no effect on fluorescence if TMPD is efficient at oxidizing reduced PQ, as the PQ pool should remain oxidized. However, exactly the opposite effect was observed: a large quenching of fluorescence was induced upon TMPD

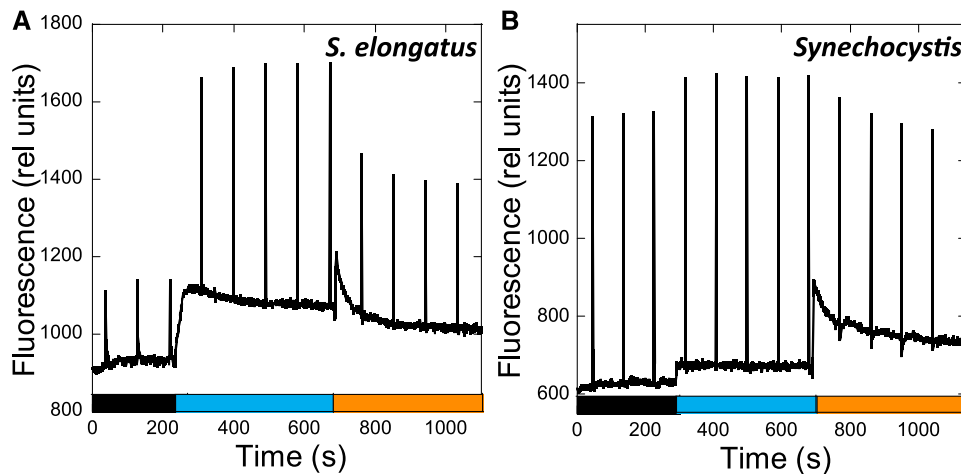


**Figure 5.** State Transitions in *S. elongatus* (A) and *Synechocystis* (B).

The fluorescence changes were followed with a PAM fluorometer. Dark-adapted cells (Chl concentration  $2.5 \mu\text{g}/\text{mL}$ ) were successively illuminated with blue light ( $85 \mu\text{M photons m}^{-2} \text{s}^{-1}$ ) and orange light ( $20 \mu\text{M photons m}^{-2} \text{s}^{-1}$ ). Saturating pulses ( $400 \text{ ms} \times 1200 \mu\text{M photons m}^{-2} \text{s}^{-1}$ ) were applied every 90 s.

addition. The amplitude of quenching depended on the TMPD concentration (Supplemental Figures 4A to 4D). This effect can be explained by assuming that, under these conditions, TMPD is primarily involved in cyclic electron transport and functions poorly as an oxidizer of reduced PQ. Cyclic electron transport also limits linear electron flow through *cyt b<sub>6</sub>f* and consequently contributes to PQ reduction. In accordance with the poor efficiency of TMPD in oxidizing reduced PQ under these conditions, the addition of TMPD to DBMIB-poisoned cells led to no change in fluorescence, indicating that State II was maintained (Supplemental Figure 4E). In addition, TMPD did not hinder the effect of DBMIB on state transitions: large fluorescence quenching was observed even in the presence of TMPD (Supplemental Figure 4F).

In an attempt to modify the behavior of TMPD, we added methyl viologen (MV) to the reaction. MV is a good electron acceptor from PSI that could compete with TMPD at this level. This approach was found to be successful: the addition of DBMIB following that of TMPD led to only a small decrease in fluorescence, indicating that under these conditions, TMPD was efficient at performing electron uptake from the PQ pool (Supplemental Figure 4G). Notably, the presence of MV did not affect state transitions in the absence of TMPD (Supplemental Figures 4F and 4G).

More importantly, when TMPD was added in the presence of MV to largely quenched DBMIB-poisoned cells, it induced a large increase in fluorescence related to the transition to State 1 (Figure 10). The final  $F_v$  was 70% that of cells under blue light illumination in the absence of chemicals. The transition to State 1 induced by TMPD under blue light illumination was larger than that induced by DMBQ in darkness (55%). Thus, TMPD is able to reverse the effect of DBMIB by taking electrons from PQ and giving them to PSI, bypassing the inhibited *cyt b<sub>6</sub>f* complex. Similar results were obtained with *Synechocystis* cells using 3 mM MV and  $7.5 \mu\text{M}$  TMPD (Figure 10). In conclusion, the transition to State I can be induced even when *cyt b<sub>6</sub>f* is inhibited by DBMIB by partially oxidizing the PQ pool.

#### Are Protein Phosphorylation Reactions Required for Cyanobacterial State Transitions?

In plants and green algae, conformational changes induced in the *cyt b<sub>6</sub>f* complex (especially in the Rieske protein) by the

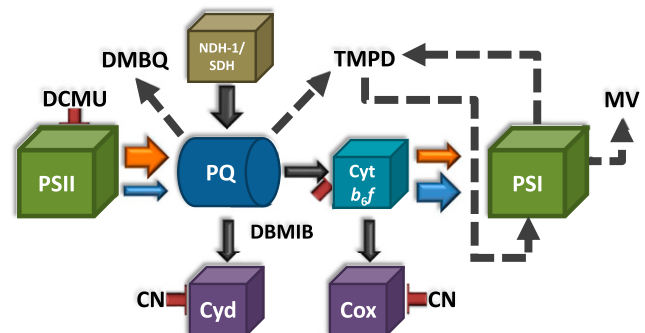


**Figure 6.** Schematic Model of the Effects of Different Chemicals on the Intersystem Electron Transport Chain in Cyanobacteria.

The arrows indicate the direction of electron transport between different protein complexes/chemical compounds. The size of each arrow is proportional to the quantity of electron transfer under different conditions. Orange and blue arrows indicate electron transfer under orange or blue light illumination, respectively. Black solid arrows indicate electron transfer occurring under dark and light conditions. Dashed arrows indicate electrons taken/given by the added chemicals. Red lines indicate the inhibition of the different complexes by the given chemicals. Protein complexes: PSII, photosystem II; PSI, photosystem I; PQ, plastoquinone pool; *Cyt b<sub>6</sub>f*, cytochrome *b<sub>6</sub>f*; NDH-1, NAD(P)H dehydrogenase type 1; SDH, succinate dehydrogenase; *Cyd*, cytochrome *bd*-type quinol oxidase; *Cox*, cytochrome *c* oxidase. Chemical compounds: DCMU, 3-(3,4-dichlorophenyl)-1,1-dimethylurea; DMBQ, 2,6-dimethoxy-1,4-benzoquinone; DBMIB, 2,5-dibromo-3-methyl-6-isopropyl-*p*-benzoquinone; TMPD, *N, N, N', N'*-tetramethyl-*p*-phenylenediamine; MV, methyl viologen; CN, cyanide.



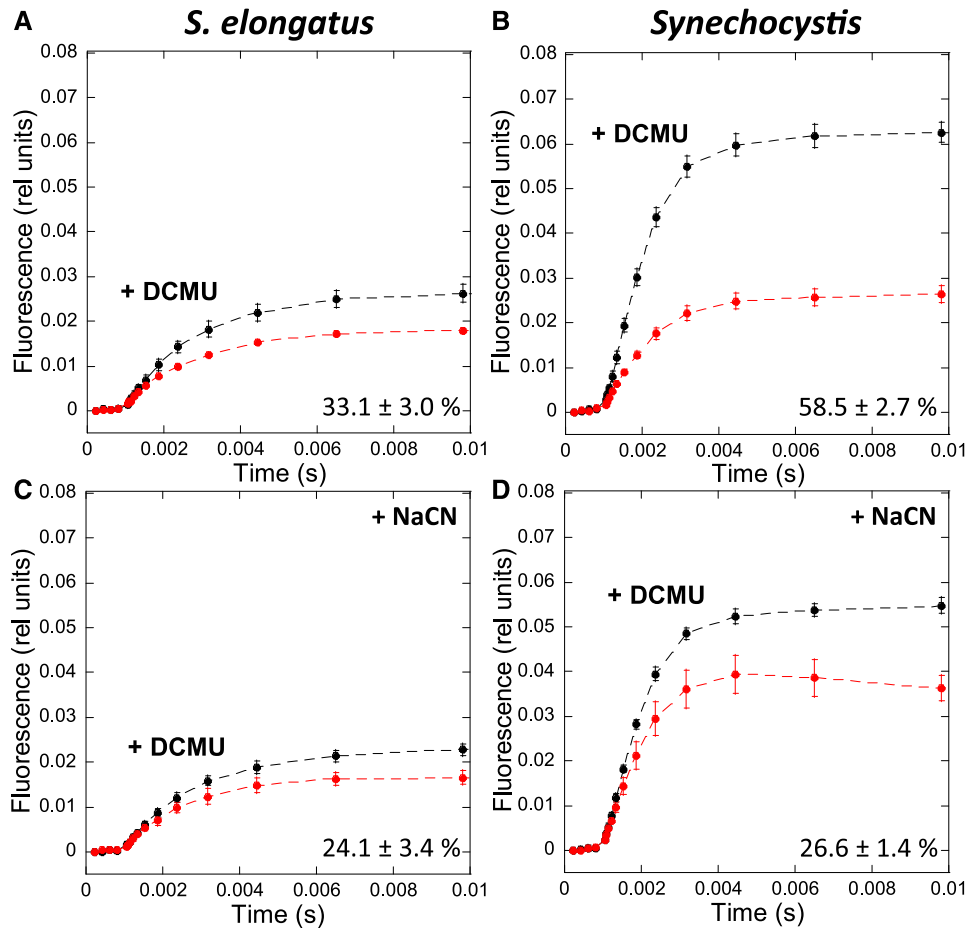


**Figure 7.** Fluorescence Induction in the Absence and Presence of NaCN in *S. elongatus* and *Synechocystis* Cells.

Whole cells (Chl concentration 2.5  $\mu\text{g}/\text{mL}$ ) were dark adapted for 15 min at 31°C before illumination with orange light (180  $\mu\text{M photons m}^{-2} \text{s}^{-1}$ ). (A) and (B) Fluorescence induction in the absence of NaCN.

(C) and (D) Fluorescence induction after 3-min incubation in the presence of NaCN (80  $\mu\text{M}$ ).

Black lines show fluorescence induction in the presence of DCMU (10  $\mu\text{M}$ ). Red lines show fluorescence induction in the absence of DCMU. The detection wavelength was  $\geq 695 \text{ nm}$  (far-red). The curves are the average of at least three independent biological replicates. The percentages shown are the area between the curves relative to the area under the curve with DCMU. The errors bars correspond to the *sd* of the data shown.

occupancy of the  $Q_D$  site by a  $\text{PQH}_2$  molecule (Zhang et al., 1998; Zito et al., 1999; Breyton, 2000; Finazzi et al., 2001) activates a specific kinase (STN7/Stt7; Depège et al., 2003; Bellaïfio et al., 2005), which phosphorylates the mobile trimers of LHCII, inducing their detachment from PSII. As previously mentioned, at least two studies suggested that protein phosphorylation by one specific Ser/Thr kinase could also trigger cyanobacterial state transitions (Allen et al., 1985; Chen et al., 2015). To test this hypothesis, we created *Synechocystis* protein kinase and phosphatase mutants. *Synechocystis* has 12 genes encoding putative Ser/Thr kinases (SPTKs). Seven of these genes encode proteins belonging to the Ser/Thr-protein kinase N2 subfamily (spkA to spkG) and five belonging to the ATP-binding cassette transporter1 subfamily (spkH to spkL; Zorina, 2013). Each gene was individually deleted by replacing it with a kanamycin resistance cassette (see Methods for details). We also individually deleted genes encoding nine phosphatases: slr0328 (Protein

tyrosine phosphatase family), slI1771, slr1860, slI1033, slI0602, slr0114, slr1983 (protein phosphatase  $\text{Mg}^{2+}$ - or  $\text{Mn}^{2+}$ -dependent family), slI1387 (phosphoprotein phosphatase family) and slr0946. Thus, we created 12 single *Synechocystis* kinase mutants and 9 single *Synechocystis* phosphatase mutants. To determine if the mutants were affected in state transitions, we illuminated dark-adapted mutant cells with blue light to induce the transition to State I, followed by orange light to induce the transition to State II (Figure 11). All of the dark-adapted single mutants went to State I upon blue light illumination and then to State II during orange light illumination (Figure 11; Supplemental Figure 5). The rates of decrease in fluorescence during the State I to State II transition were similar in the wild-type and mutant cells (Figure 11; Supplemental Figure 5). These experiments indicate that no specific Ser/Thr kinase or phosphatase is involved in cyanobacterial state transitions, as it is the case in green algae and plants.

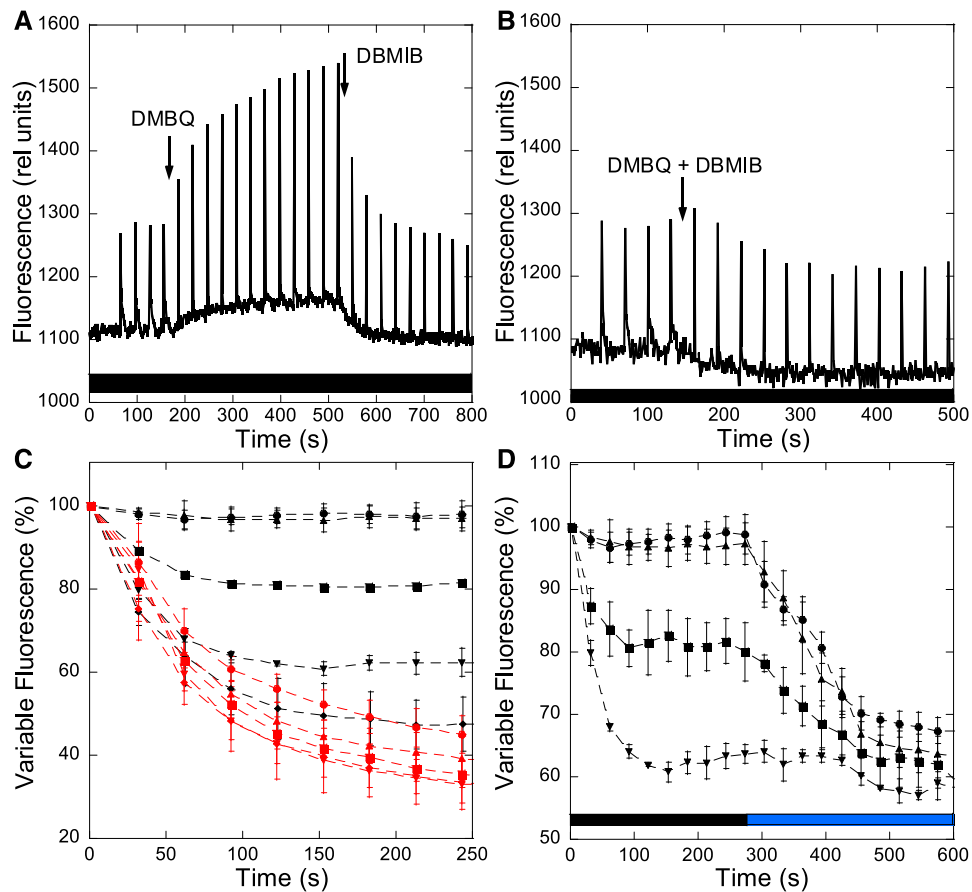


**Figure 8.** Fluorescence Changes Induced by Chemicals.

*S. elongatus* cells were dark adapted (15 min) before the successive addition of DMBQ (250  $\mu\text{M}$ ) and DBMIB (20  $\mu\text{M}$ ) (A) or the simultaneous addition of DMBQ (250  $\mu\text{M}$ ) and DBMIB (20  $\mu\text{M}$ ) (B). The measurements were done using a PAM fluorometer (measuring light 650 nm). Saturating pulses (400 ms  $\times$  1200  $\mu\text{M}$  photons  $\text{m}^{-2}$   $\text{s}^{-1}$ ) were applied every 30 s. Typical experiments are shown.

(C) Variable fluorescence traces of different concentrations of DBMIB, added at time 0, when State I was induced by blue light (red lines, 85  $\mu\text{M}$  photons  $\text{m}^{-2}$   $\text{s}^{-1}$ ) or by DMBQ (250  $\mu\text{M}$ ) in darkness (black lines). The values were normalized to the variable fluorescence of State I (induced by light or DMBQ, respectively).

(D) Variable fluorescence traces of different concentrations of DBMIB when State I was induced by DMBQ (250  $\mu\text{M}$ ) in darkness, and the cells were then illuminated with blue light (85  $\mu\text{M}$  photons  $\text{m}^{-2}$   $\text{s}^{-1}$ ). The values were normalized to the variable fluorescence of State I induced by DMBQ.

The averages of at least three independent biological replicates are shown. The errors bars correspond to the SD of the data shown. (●) 2.5  $\mu\text{M}$  DBMIB; (▲) 5  $\mu\text{M}$  DBMIB; (■) 10  $\mu\text{M}$  DBMIB; (▼) 15  $\mu\text{M}$  DBMIB; (◆) 20  $\mu\text{M}$  DBMIB.

To confirm that phosphorylation reactions are not essential for cyanobacterial state transitions, we tested the effects of kinase and phosphatase inhibitors on *Synechocystis* and *S. elongatus*. Staurosporine and K252a (a derivative of staurosporine) are potent inhibitors of Ser/Thr and Tyr kinases that interact with their ATP binding sites (Fernandez et al., 2006; Nakano and Omura, 2009). NaF inhibits Ser/Thr and acid phosphatases and  $\text{Na}_3\text{VO}_4$  inhibits Tyr and alkaline phosphatases (Delphin et al., 1995; McCartney et al., 1997; and references inside). Staurosporine and NaF were shown to inhibit state transitions in the green alga *Chlamydomonas reinhardtii* (Delphin et al., 1995 and references inside). Figure 12 shows that the presence of staurosporine or K252a, which were added in excess (21  $\mu\text{M}$  and 1  $\mu\text{M}$ , with the half maximal inhibitory concentration of these compounds 0.6  $\mu\text{M}$  and

96 nM, respectively (Nakano and Omura, 2009) did not inhibit state transitions in *Synechocystis* or *S. elongatus*.

To confirm that these kinase inhibitors are able to enter cyanobacterial cells and inhibit phosphorylation reactions, we tested their effects on the phosphorylation of the  $\text{P}_{\text{II}}$  protein in *S. elongatus*. The  $\text{P}_{\text{II}}$  protein (*glnB* gene product) is involved in the tight coordination of carbon and nitrogen assimilation. Its activity involves the phosphorylation and dephosphorylation of a Ser residue (Forchhammer and Tandeau de Marsac, 1995a, 1995b). In ammonium-grown cells,  $\text{P}_{\text{II}}$  is completely dephosphorylated. The transfer of cells to medium lacking combined nitrogen induces phosphorylation of  $\text{P}_{\text{II}}$  (Forchhammer and Tandeau de Marsac, 1995a, 1995b). The phosphorylation state of  $\text{P}_{\text{II}}$  can be analyzed by gel electrophoresis in a phos-tag gel SDS-PAGE system and by

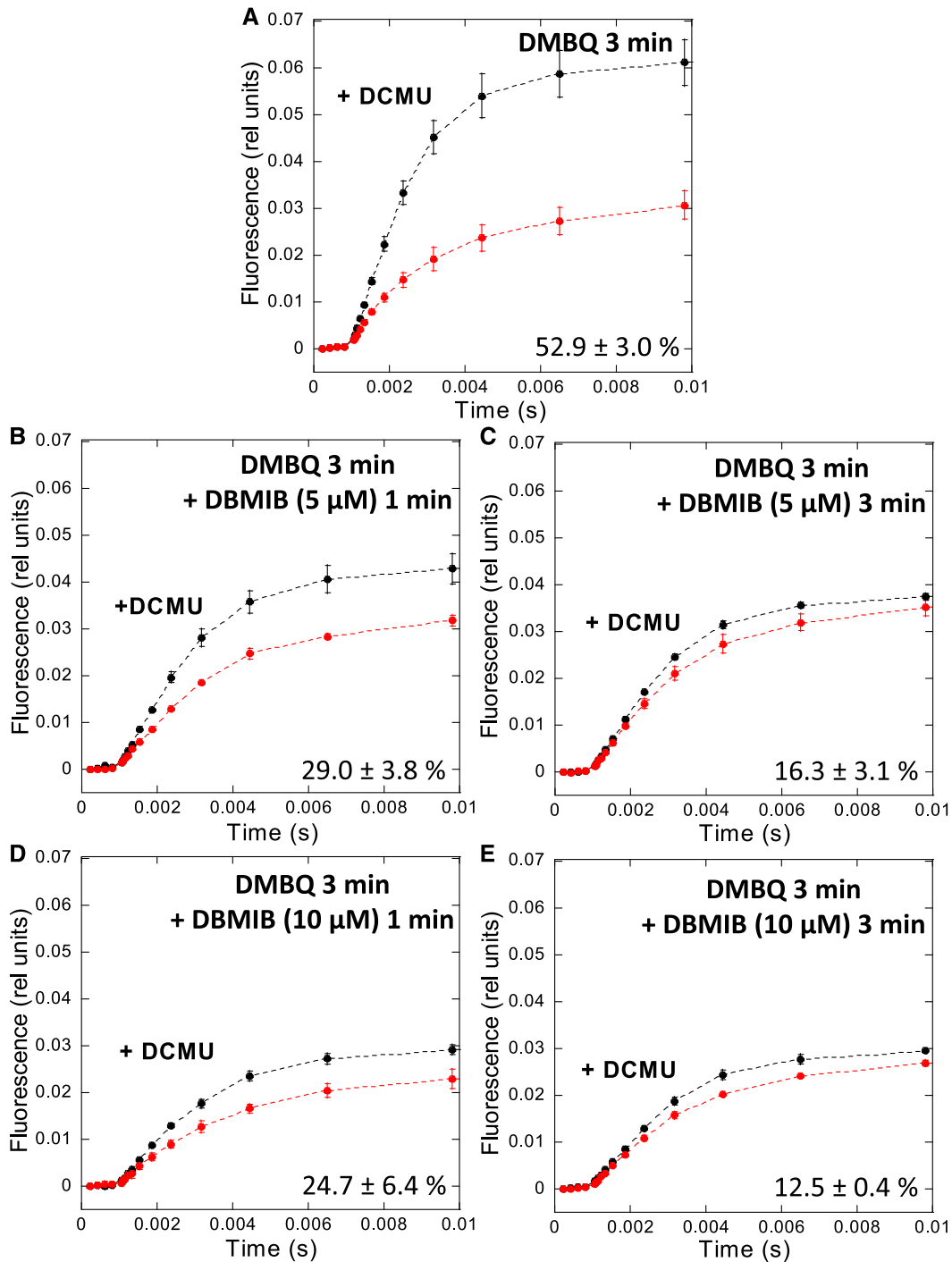


**Figure 9.** Estimation of the PQ Pool Redox State.

Fluorescence induction in the presence (black lines) or absence (red lines) of DCMU (10 μM) in dark-adapted *S. elongatus* cells. Whole cells (Chl concentration 2.5 μg/mL) were dark adapted for 15 min (at 31°C) before illumination with orange light (180 μM photons m<sup>-2</sup> s<sup>-1</sup>).

**(A)** Cells were incubated for 3 min with DMBQ (250 μM).

**(B)** and **(C)** Cells were incubated with DMBQ (250 μM) for 3 min and then with DBMIB (5 μM) for 1 min or 3 min, respectively.

**(D)** and **(E)** Cells were incubated with DMBQ (250 μM) for 3 min and then with DBMIB (10 μM) for 1 min or 3 min, respectively.

Black lines show fluorescence induction in the presence of DCMU. Red lines show fluorescence induction in the absence of DCMU. The detection wavelength was ≥695 nm (far-red). The curves are the average of at least three independent biological replicates. The percentages shown are the area between the curves relative to the area under the curve with DCMU. The errors bars correspond to the *sd* of the data shown.

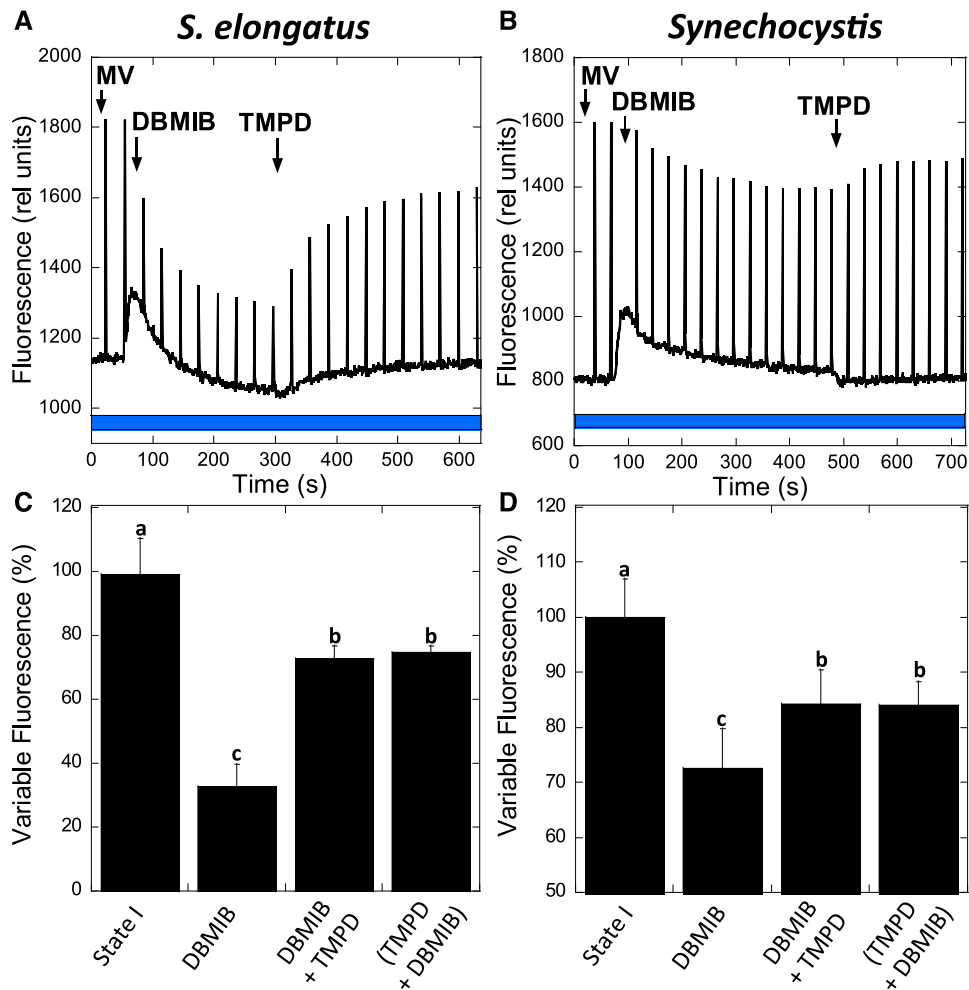


**Figure 10.** Fluorescence Changes Induced by TMPD in the Presence of MV and DBMIB.

*S. elongatus* (A) and *Synechocystis* (B) cells were dark adapted (15 min) before the transition to State I by blue light illumination ( $85 \mu\text{M photons m}^{-2} \text{s}^{-1}$ ) in the presence of MV (2 mM or 3 mM, respectively). DBMIB ( $10 \mu\text{M}$  for *S. elongatus* or  $7.5 \mu\text{M}$  for *Synechocystis*) was then added. After reaching a steady State II, TMPD ( $10 \mu\text{M}$ ) was added. Saturating pulses were applied every 30 s.

(C) and (D) Graphs show the percentage of variable fluorescence for *S. elongatus* and *Synechocystis*, respectively, after blue light illumination (State I); after the addition of DBMIB; DBMIB and then TMPD or when both chemicals were added at the same time.

The mean and SD of four independent biological replicates are shown. Columns without common letters differ significantly (Tukey test,  $P < 0.05$ ).

immunoblot detection. In this system, phosphorylated proteins migrate more slowly than non-phosphorylated ones (Kinoshita and Kinoshita-Kikuta, 2011). Figure 12G shows that the presence of staurosporine and K252a completely inhibited the phosphorylation of the  $P_{II}$  protein under nitrogen starvation conditions. This result indicates that both kinase inhibitors entered into *S. elongatus* cells and were able to inhibit protein phosphorylation.

Finally, phosphatase inhibitors (NaF and  $\text{Na}_3\text{VO}_4$ ) also did not affect state transitions (Figure 13). Nevertheless, NaF induced the partial inhibition of the oxygen-evolving activity of PSII (Supplemental Figure 6) and a general decrease in fluorescence (Figure 13) in *Synechocystis*, indicating that this chemical entered the cells. In conclusion, our experiments show that phosphorylation reactions are not involved in cyanobacterial state transitions.

## DISCUSSION

While the mechanism of state transitions in plants and green algae has been largely elucidated, it remains to be characterized in cyanobacteria. Contradictory hypotheses have been proposed about cyanobacterial state transitions based on studies addressing different aspects of the mechanism: the movement of PBS, spillover, reorganization of membrane complexes, involvement of *cyt b<sub>6</sub>f*, and/or phosphorylation reactions in signal transduction. However, none of these hypotheses has been definitively supported. Our results help to elucidate open questions about the mechanism behind the large fluorescence quenching observed in State II and the alleged role of the *cyt b<sub>6</sub>f* complex in the signaling pathway involved in cyanobacterial state transitions.

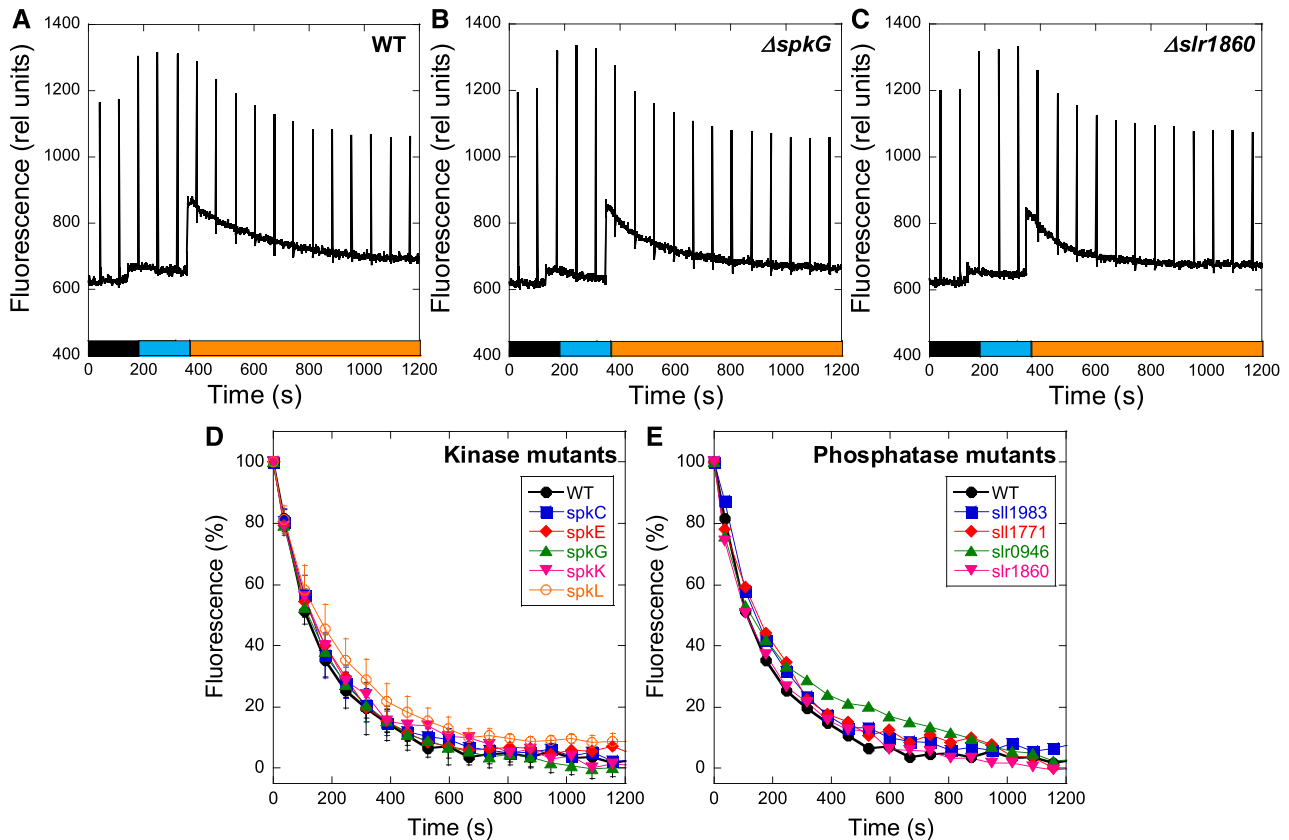


**Figure 11.** State Transitions in *Synechocystis* Kinase and Phosphatase Mutants.

The fluorescence changes were followed with a PAM fluorometer. Dark-adapted cells (Chl concentration  $2.5 \mu\text{g}/\text{mL}$ ) were successively illuminated with blue light ( $85 \mu\text{M photons m}^{-2} \text{s}^{-1}$ ) and orange light ( $40 \mu\text{M photons m}^{-2} \text{s}^{-1}$ ). Typical experiments are shown for the *Synechocystis* wild-type (WT) (A),  $\Delta spkG$  (B), and  $\Delta slr1860$  (C) cells. Saturating pulses ( $400 \text{ ms} \times 1200 \mu\text{M photons m}^{-2} \text{s}^{-1}$ ) were applied every 70 s.

(D) and (E) Variable fluorescence (%) decrease induced by orange illumination of blue light-adapted cells (State I to State II transition) of kinase and phosphatase mutants, respectively. The values were normalized, with the variable fluorescence of State I equal to 100% and the variable fluorescence of State II equal to 0%.

(D) The values for the wild type (WT) and  $\Delta spkC$ ,  $\Delta spkE$ ,  $\Delta spkG$ ,  $\Delta spkK$ , and  $\Delta spkL$  mutants are shown.

(E) The values for the wild type (WT) and  $\Delta slr1983$ ,  $\Delta slr1771$ ,  $\Delta slr0946$ , and  $\Delta slr1860$  mutants are shown.

The averages of at least three independent biological replicates are shown. The errors bars correspond to the sd of the data shown.

### The Contributions of PBS Versus the Membrane to State Transitions

It was previously shown that PBS can easily move and that high concentrations of betaine, Suc, and phosphate inhibit the diffusion of PBS and state transitions (Joshua and Mullineaux, 2004; Li et al., 2004, 2006). Li et al. (2004) also observed that, in *Spirulina platensis*, betaine inhibits changes in 77 K emission spectra with 430 nm excitation. However, the authors did not discuss this last result. Based on these works, it was concluded that the movement of PBS from one photosystem to the other was the main reason for the observed changes in fluorescence. By contrast, we demonstrated that these chemicals, in addition to hindering PBS movement, inhibit fluorescence changes that depend on membrane processes. No fluorescence change in 77 K emission spectra was detected in the presence of betaine, Suc, or phosphate upon cells' illumination, not only when PBSs were excited but also when Chl was excited. Thus, based on these experiments,

it cannot be concluded that the movement of PBS is the main contributor to state transitions in cyanobacteria.

Our experiments did not allow us to distinguish which changes, if any, occur at the level of PBS during state transitions: detachment of PBS from one or both photosystems, or changes in energy transfer from PBS to one or the other photosystem. Nevertheless, we expect the contribution of these changes to be small in both *S. elongatus* and *Synechocystis*, because the main increase in fluorescence emission from State II to State I was related to PSII (G3, 695 nm emission peak; Supplemental Figures 1 and 2).

### PSII Quenching Is Involved in State II

Ranjbar Choubeh et al. (2018) recently showed that state transitions involve a reversible quenching of PSII fluorescence independently of spillover changes in *S. elongatus* cells. They



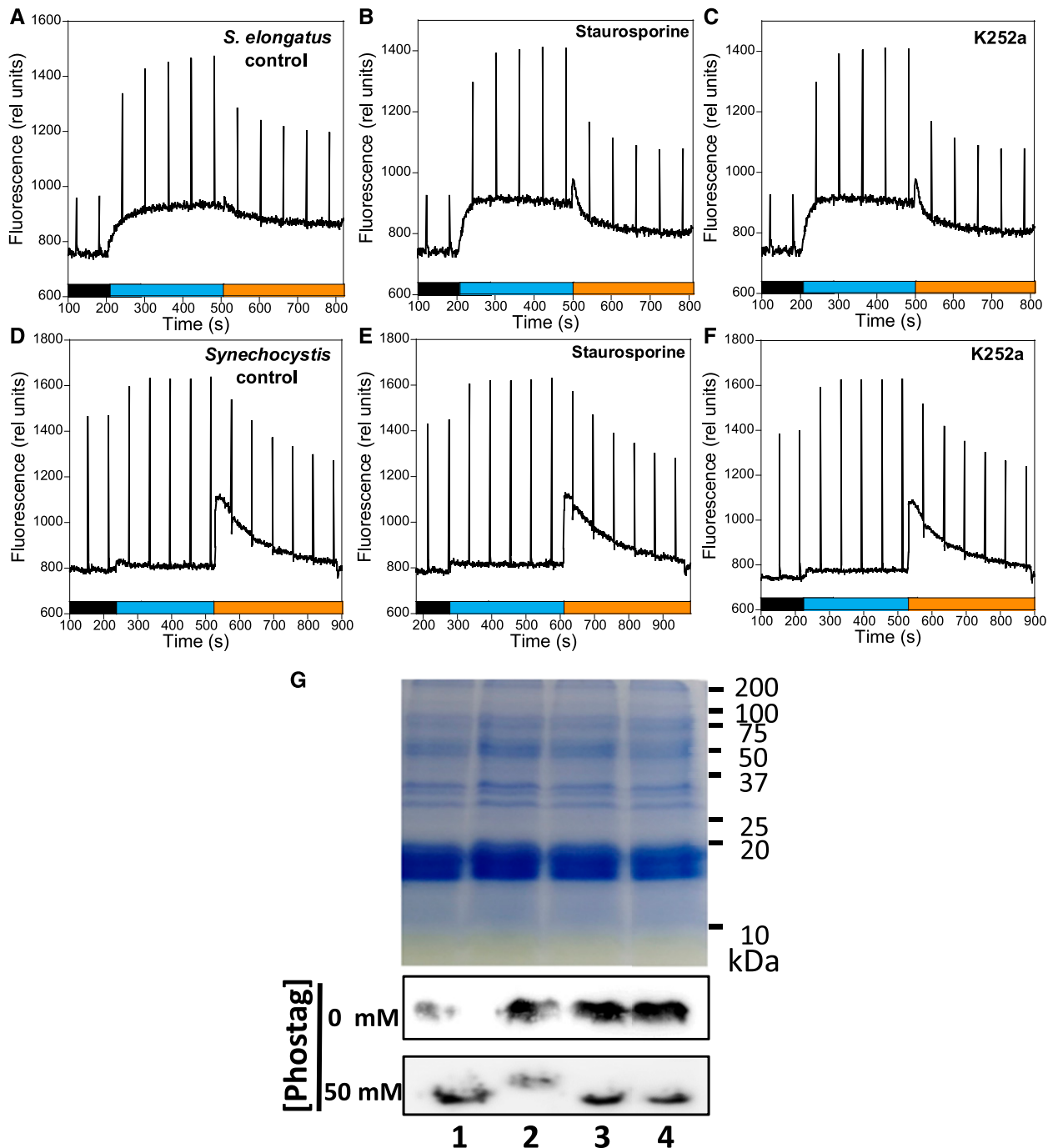


**Figure 12.** Effects of Kinase Inhibitors on State Transitions and PII Phosphorylation.

*S. elongatus* (A) to (C) and *Synechocystis* (D) to (F) cells were incubated in the absence and presence of kinase inhibitors for 90 min in darkness. Then the cells (Chl concentration  $2.5 \mu\text{g}/\text{mL}$ ) were successively illuminated with blue light ( $85 \mu\text{M photons m}^{-2} \text{s}^{-1}$ ) and orange light ( $40 \mu\text{M photons m}^{-2} \text{s}^{-1}$ ), and the fluorescence changes were followed using a PAM fluorometer.

(A) and (D) Control cells containing DMSO (0.1% v/v).

(B) and (E) Cells treated with staurosporine ( $21 \mu\text{M}$ ).

(C) and (F) Cells treated with K252a ( $1.07 \mu\text{M}$ ). Saturating pulses ( $400 \text{ ms} \times 1200 \mu\text{M photons m}^{-2} \text{s}^{-1}$ ) were applied every 60 s.

(G) Gel electrophoresis containing Phos-tag to detect phosphorylated proteins and immunoblot using an anti-PII protein. (1) BG11 medium; (2) nitrogen-depleted BG11 medium; (3) nitrogen-depleted BG11 medium supplemented with K252a ( $1.07 \mu\text{M}$ ); (4) nitrogen-depleted BG11 medium supplemented with staurosporine ( $21 \mu\text{M}$ ).

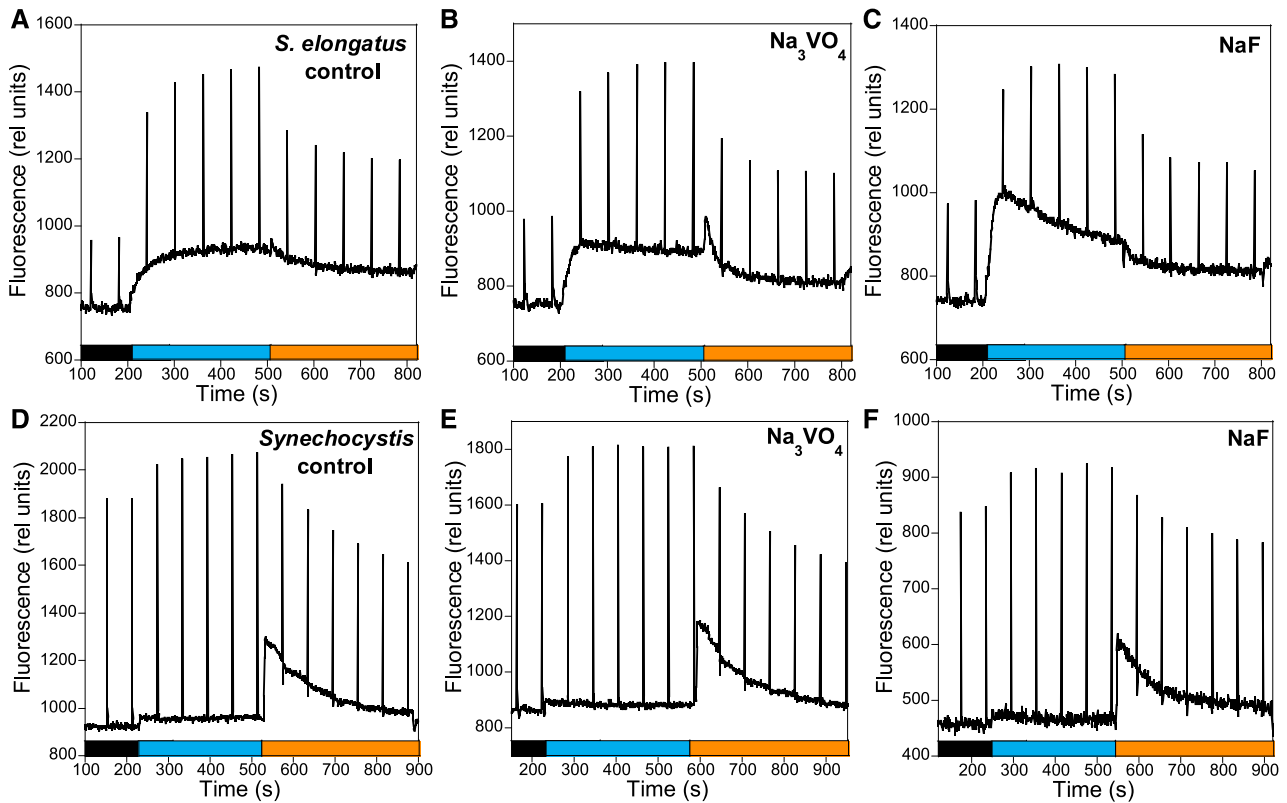


**Figure 13.** Effect of Phosphatase Inhibitors on State Transitions.

*S. elongatus* (A) to (C) and *Synechocystis* (D) to (F) cells were incubated in the absence and presence of phosphatase inhibitors for 90 min in darkness. Then the cells (Chl concentration 2.5  $\mu\text{g}/\text{mL}$ ) were successively illuminated with blue light (85  $\mu\text{M}$  photons  $\text{m}^{-2} \text{s}^{-1}$ ) and orange light (40  $\mu\text{M}$  photons  $\text{m}^{-2} \text{s}^{-1}$ ) and the fluorescence changes were followed using a PAM fluorometer.

(A) and (D) Control cells containing NaCl (100 mM).

(B) and (E) Cells treated with  $\text{Na}_3\text{VO}_4$  (1 mM).

(C) and (F) Cells treated with NaF (50 mM). Saturating pulses (400 ms  $\times$  1200  $\mu\text{M}$  photons  $\text{m}^{-2} \text{s}^{-1}$ ) were applied every 60 s.

measured the fluorescence decay kinetics of cells in State II and State I with a streak camera using 430 nm or 577 nm excitation at 77 K. By performing global analysis of the data, the authors obtained decay-associated spectra. When 430 nm excitation was used, PSII emission decreased, but the decay-associated spectra showed that PSI emission was similar in State I and State II. This argues against a change in spill-over during state transitions. This was also observed in *Synechocystis* cells (Ranjbar Choubbeh et al., 2018).

Our results confirm these observations. We showed that both the 683 nm and 695 nm peaks decrease in State II (under Chl and PBS excitation), whereas the 718 nm peak did not change (see Supplemental Figures 1 and 2, including peak deconvolution to visualize different components of the spectra). The absence of changes in PSI-related fluorescence during state transitions was confirmed by normalizing the spectra with an external dye (Rhodamine B; Figure 3). These results indicate that PSII emission is largely quenched in State II and that spillover from PSII to PSI does not contribute to this quenching. The PSII-related quenching mechanism remains to be elucidated.

### The Role of Cyt *b<sub>6</sub>f* in Cyanobacterial State Transitions

One of the big questions that remain to be answered about the mechanism of cyanobacterial state transitions is how the signal is transmitted from the PQ pool to the PBS and/or photosystems to induce their movements or fluorescence quenching. In plants and green algae, the binding (and subsequent release) of  $\text{PQH}_2$  in the  $\text{Q}_o$  site of the cyt *b<sub>6</sub>f* complex plays a critical role in the activation of a specific Ser/Thr kinase that phosphorylates LHCII (Vener et al., 1995, 1997; Zito et al., 1999). The phosphorylated LHCII detaches from PSII and totally (or partially) associates with PSI (Vener et al., 1997; Wollman, 2001). The role of the  $\text{Q}_o$  site in state transitions was first suggested based on the effect of DBMIB in *Chlamydomonas*, where DBMIB inhibits State I to State II transition, although in its presence, the PQ pool is largely reduced (Finazzi et al., 2001). By contrast, in cyanobacteria, DBMIB induces the State I to State II transition. This occurs even in the presence of DCMU (which inhibits photoreduction of the PQ pool by PSII) or DMBQ (which oxidizes the PQ pool by taking electrons from  $\text{PQH}_2$ , as shown in present results and in Mao et al. [2002] and Huang et al. [2003]). These authors proposed that the action of DBMIB is

related to its binding to the  $Q_o$  site and not to the reduction of the PQ pool. The authors assumed that the PQ pool remains oxidized in the presence of both DBMIB and DMBQ (or PBQ).

Here, we demonstrated that this is not true, because the addition of DBMIB induced reduction of the PQ pool even in the presence of DMBQ. Moreover, we demonstrated that the same concentration of DBMIB has different effects on state transitions depending on the experimental conditions. For instance, DBMIB at 5  $\mu$ M was unable to induce the transition to State II in dark-adapted cells in the presence of DMBQ, whereas it induced large quenching in blue-green-light-adapted cells in the absence or presence of DMBQ. The amplitude of fluorescence quenching induced by 10  $\mu$ M DBMIB was also larger under illumination than in darkness in the presence of DMBQ. Altogether, these experiments strongly suggested that the *cyt b<sub>6</sub>f* complex is not involved in cyanobacterial state transitions. The finding that the addition of TMPD to DBMIB-poisoned cells induced a large increase in fluorescence related to PQ oxidation and transition to State I indicates that DBMIB binding to the  $Q_o$  site of *cyt b<sub>6</sub>f* is not involved in the transition to State II. Under these conditions, DBMIB remained attached to the  $Q_o$  site, and the *cyt b<sub>6</sub>f* complex was inactive. As an alternative, it was recently proposed that the single Chl *a* molecule present in *cyt b<sub>6</sub>f* could act as a redox sensor and signal transmitter during state transitions (Vladkova, 2016). This Chl *a* molecule is evolutionarily conserved and is present in all oxygen-evolving photosynthetic species (Vladkova, 2016). However, changes in this Chl *a* were induced by binding of DBMIB or PQH<sub>2</sub> to the  $Q_o$  site. Thus, based on our results, the involvement of this Chl *a* molecule in cyanobacterial state transitions is not likely.

In addition, the characterization of 12 kinase and 9 phosphatase single mutants demonstrated that no specific protein kinase and/or phosphatase is necessary for cyanobacterial state transitions. More generally, the use of kinase and phosphatase inhibitors demonstrated that phosphorylation reactions are not essential for state transitions in *Synechocystis* and *S. elongatus*. Thus, signal transduction from the PQ pool to the antenna and the photosystems is completely different in cyanobacteria versus green algae and plants.

While DCMU and DBMIB have opposite effects on cyanobacterial state transitions, they have the same effect on the transcription of photosynthetic genes (Alfonso et al., 1999, 2000; El Bissati and Kirilovsky, 2001). Both DCMU and DBMIB induced an increase in *psbA* transcription and a decrease in *psaE* transcription when added into *Synechocystis* cells under white and orange illumination. These findings strongly suggest that *cyt b<sub>6</sub>f* is involved in the redox transcriptional regulation of photosynthetic genes in *Synechocystis* (Alfonso et al., 1999, 2000; El Bissati and Kirilovsky, 2001). In conclusion, *cyt b<sub>6</sub>f* is not involved in cyanobacterial state transitions, but it appears to be involved in redox transcriptional regulation.

Because it seems that in cyanobacteria, the principal effect of PQ reduction is an increase in PSII quenching and that *cyt b<sub>6</sub>f* is not involved in the signaling pathway, it is tempting to hypothesize that PSII itself senses the redox state of the PQ pool. Sensing cannot be linked to  $Q_A^-$  accumulation because both the presence of DCMU and the reduction of the PQ pool increase  $Q_A^-$  concentration; but while DCMU induces the transition to State I, the

reduction of the PQ pool induces the transition to State II. DCMU binding and over-reduction of the PQ pool were previously found to accelerate photoinhibition but through different mechanisms (Kirilovsky et al., 1994; Fufezan et al., 2005; Fischer et al., 2006). In line with this observation, the  $Q_B$  site could be modified differently in the presence of DCMU or PQH<sub>2</sub>, leading to different effects on  $Q_A$  redox potential, recombination reactions, and the generation of PSII quenching related to State II.

The PQ pool redox state could be sensed not only at the level of the  $Q_B$  site but also by the  $Q_C$  hydrophobic tunnel. The existence of this  $Q_C$  tunnel formed by *cyt b559* and *psbJ* was suggested by the x-ray crystallographic structural model of PSII of *Thermosynechococcus elongatus* at 2.9 Å resolution (Guskov et al., 2009). The function of this tunnel as a quinone binding site remains to be confirmed, because later structures at higher resolution did not contain a quinone in this hydrophobic pocket (Umena et al., 2011). However, *Synechocystis* mutants containing mutations around the proposed  $Q_C$  site show altered state transitions, making this site another interesting target of study (Huang et al., 2016).

In addition of these  $Q_{B/C}$  sites, there are other ways by which the redox state of the PQ pool could be sensed; the participation of other known proteins or novel factors in the signaling pathway cannot be ruled out. Overall, while the PSII-quenching mechanism and the redox sensor of the PQ pool remain to be elucidated, our results rule out the involvement of *cyt b<sub>6</sub>f* in this process.

## METHODS

### Culture Conditions and Replicates

The cyanobacteria *Synechocystis* PCC 6803 and *Synechococcus elongatus* PCC 7942 strains were grown photo-autotrophically in blue-green (BG11) medium (Herdman et al., 1973). The cells were incubated in a rotary shaker (120 rpm) at 31°C illuminated by fluorescence white lamps (50  $\mu$ M photons  $m^{-2} s^{-1}$ ) under a CO<sub>2</sub>-enriched atmosphere. The cells were maintained in their logarithmic phase of growth for all experiments. The kinase and phosphatase mutants were grown in the presence of kanamycin (40  $\mu$ g/mL).

A biological replicate is a batch of cells on a particular day. The measurements were performed several times using the same batch of cells (technical replicates). The mean of each batch was calculated. The biologically independent experiments were performed on different days separated by at least a week. Thus, completely different cells were tested.

### Construction of Kinase and Phosphatase Mutants

To obtain the kinase mutants ( $\Delta$ *spkB*,  $\Delta$ *spkD*,  $\Delta$ *spkE*,  $\Delta$ *spkF*,  $\Delta$ *spkG*,  $\Delta$ *spkI*,  $\Delta$ *spkJ*,  $\Delta$ *spkK*, and  $\Delta$ *spkL*) a 500 bp fragment in the upstream region of each kinase gene was cloned into the pMD T-18 vector (Takara, Japan) and digested with XbaI. The PRL446 plasmid containing the kanamycin cassette was also digested with XbaI. Both linear fragments were ligated to generate the plasmid use to transform the *Synechocystis* wild-type cells in order to obtain the knockout kinase mutants. The strategy to obtain the  $\Delta$ *spkA* and the  $\Delta$ *spkC* mutants was similar with only two minor modifications: 1) the plasmid containing the 500 bp upstream fragment was digested with SmaI instead of XbaI. 2) To obtain the final construction, the linearized plasmid was ligated to the kanamycin cassette with blunt ends, and the pPM-kinase-upper-kanamycin was obtained.

In parallel, a 500 bp fragment in the downstream region of each kinase gene was cloned into the pMD T-18 vector (Takara) and digested with Sall to generate the downstream fragment. Blunt ends were generated in the

downstream fragment and in the pPM-kinase-upper-kanamycin linearized using the *SacI*/*SphI* enzyme. The resulting blunt-end DNAs were ligated together. After testing the direction of the inserted downstream fragment by PCR, the pPM-kinase-upper-kanamycin-down was used to transform the wild-type *Synechocystis* cells.

To obtain the phosphatase mutants ( $\Delta$ *slr0328*,  $\Delta$ *slr1771*,  $\Delta$ *slr1860*,  $\Delta$ *slr1033*,  $\Delta$ *slr0602*,  $\Delta$ *slr0114*,  $\Delta$ *slr1983*,  $\Delta$ *slr1387*, and  $\Delta$ *slr0946*), a 500 bp fragment upstream of each phosphatase gene, the kanamycin cassette, and a 500 bp fragment downstream of each phosphatase gene were spliced together using the PCR overlap extension method to obtain the upper-kanamycin-down DNA fragment for each phosphatase gene. The resulting DNA fragments were supplemented with a thymine at both termini and inserted into the T-cloning vector pMD T-18 (Takara) to generate the final pPM-phosphatase-upper-kanamycin-down plasmids.

The *Synechocystis* wild-type cells were transformed with these plasmids to obtain the knockout kinase and phosphatase mutants. The presence of the kanamycin cassette replacing the kinase and phosphatase genes and the complete segregation of each mutant were tested by PCR amplification and sequencing.

The oligonucleotides used in these constructions are described in Supplemental Table.

The  $\Delta$ *spkH* *Synechocystis* mutant construction is described in (Zorina et al., 2011).

## Fluorescence Measurements

### PAM Fluorometer

State transitions were monitored using a pulse amplitude modulated fluorometer (101/102/103-PAM; Walz) in a  $1 \times 1$ -cm square stirred cuvette. All experiments were performed at 31°C on dark-adapted (15 min) whole cells at a Chl concentration of 2.5  $\mu$ g/mL. State I was induced by treatment with 85  $\mu$ M photons  $m^{-2} s^{-1}$  of blue-green light (halogen white light filtered by a Corion cut-off 550-nm filter, 400 to 500 nm). State II was induced by treatment with 25 (or 40)  $\mu$ M photons  $m^{-2} s^{-1}$  of orange light (halogen white light filtered by a Melles Griot 03 FIV 046 filter, 600 to 640 nm) or by dark incubation. Saturating flashes (400 ms  $\times$  1200  $\mu$ M photons  $m^{-2} s^{-1}$ ) were given to probe the maximum fluorescence level. The fluorescence parameters used in the analysis are the following:  $F_0$ , basal fluorescence;  $F_{md}$ , maximum fluorescence in darkness;  $F_m'$ , maximum fluorescence under illumination;  $F_{mb}'$ , maximum fluorescence under blue light illumination;  $F_{mo}'$ , maximum fluorescence under orange light illumination; variable fluorescence ( $F_v$ ) =  $F_m - F_0$ ;  $F_{vd}$ , variable fluorescence in darkness;  $F_{vb}$ , variable fluorescence under blue light illumination.

State transitions in the  $\Delta$ *spkH* mutant was measured in Turku (Finland) with a dual-PAM and compared with its own wild type. State I was induced by treatment with 50  $\mu$ M photons  $m^{-2} s^{-1}$  of blue light (460 nm) and then State II by treatment with 50  $\mu$ M photons  $m^{-2} s^{-1}$  of orange light (635 nm). The measuring light was at 620 nm.

When mentioned, 2,6-dimethoxy-1,4-benzoquinone (DMBQ, 250  $\mu$ M) and/or 2,5-dibromo-3-methyl-6-isopropyl-*p*-benzoquinone (DBMBQ, 2.5 to 20  $\mu$ M), methyl viologen (2 mM or 3 mM) or *N, N, N', N'*-tetramethyl-*p*-phenylenediamine (TMPD, 7.5 or 10  $\mu$ M) were added to the stirred cuvette.

When mentioned, staurosporine (21  $\mu$ M), K252a (1.07  $\mu$ M), NaF (50 or 100 mM) or  $Na_3VO_4$  (1 mM) were added to dark-adapted cells. The kinase inhibitors were incubated for 90 min and the phosphatase inhibitors for 1 hour. Longer incubations gave the same results. State transitions were then measured.

### PQ Pool Redox State Estimations

The PQ pool redox state was estimated by measuring fluorescence induction curves in the presence and absence of DCMU in a PSI fluorometer

(PSI Instruments). Whole cells (Chl concentration 2.5  $\mu$ g/mL) were dark-adapted for 15 min at 31°C, and illuminated (orange light 180  $\mu$ M photons  $m^{-2} s^{-1}$ ,  $\lambda = 630$  nm) in the 1-ms to 1-s time range with or without 3-(3,4-dichlorophenyl)-1,1-dimethylurea (DCMU, 10  $\mu$ M). The measuring light for these experiments was blue ( $\lambda = 460$  nm), and detection was in the far-red region ( $\geq 695$  nm). The fluorescence induction curves were followed in each case, and the area between them was considered to be proportional to the oxidation state of the PQ pool. In addition, measurements in the presence of DMBQ (250  $\mu$ M) and/or DBMBQ (5 or 10  $\mu$ M), with or without DCMU (10  $\mu$ M) were performed.

### Fluorescence Emission Spectra

We monitored 77 K fluorescence emission spectra in a CARY Eclipse spectrophotometer (Varian, Santa Clara, CA, USA). In all cases, whole cells (Chl concentration 5.0  $\mu$ g/mL) were dark-adapted for 15 min before the measurements. Then, spectra were recorded corresponding to State II. For State I spectra, cells were illuminated for 5 min with 85  $\mu$ M photons  $m^{-2} s^{-1}$  of blue-green light (halogen white light filtered by a Corion cut-off 550-nm filter; 400 to 500 nm). Samples were collected in nuclear magnetic resonance tubes and frozen by immersion in liquid nitrogen. Excitation was made at 430 nm or 590 nm, and emission was scanned from 620 nm to 800 nm. All the spectra were normalized by the signal intensity at 800 nm. When Rhodamine B (0.4  $\mu$ M) was added as an internal standard, excitation was made at 430 nm and emission was scanned from 550 nm to 800 nm. In these cases, the spectra were normalized to the Rhodamine B peak at 568 nm.

To address the effects of high osmotic buffers in state transitions, betaine (1 M), Suc (1 M), or  $K_2HPO_4/KH_2PO_4$  buffer (0.5 M, pH 7.5) was added to cells pre-adapted to State I or State II. The cells were incubated with the different buffers for 5 min, before State II or I was induced by darkness or blue light illumination (5 min), respectively. Samples were taken before and after 5-min incubation with the chemicals and at the end of the light/dark treatment. Excitation was at 430 nm or 590 nm, and emission was scanned from 620 nm to 800 nm. All of the spectra were normalized by the signal intensity at 800 nm.

### EPR Measurements

To assess the PSI/PSII ratio in the cyanobacterial strains, reduced  $F_A/F_B$  Fe-S centers and TyrD<sup>+</sup> were measured as an estimation of PSI and PSII levels, respectively. First, 300 mL of cells ( $OD_{800} = 1.0$ ) were harvested and washed with 50 mL of washing buffer [50 mM HEPES] pH 8.0, 5 mM  $MgCl_2$ ]. The cells were then centrifuged at 6000 rpm for 10 min at 20°C and washed again with 25 mL of washing buffer. This step was repeated, and the cells were washed with 2 mL of buffer. Finally, the cells were centrifuged at 3500 rpm for 10 min at 20°C and resuspended in 500  $\mu$ L of buffer.

Calibrated EPR tubes were prepared with 150  $\mu$ L of concentrated cells and 20  $\mu$ L of 200 mM potassium ferricyanide. The tubes were illuminated for 30 s and incubated in darkness for 5 s before freezing. This treatment elicited full oxidation of TyrD<sup>+</sup>, with no or very little P700<sup>+</sup> (a few percent). In case some P700<sup>+</sup> was present, its contribution was subtracted in order to obtain a pure TyrD<sup>+</sup> line shape before spin quantitation. The spectra were recorded at 20 K with an ESR300D X-band spectrometer (Bruker, Rheinstetten, Germany), using a TE<sub>102</sub> resonator equipped with a front grid for sample illumination within the cavity. Illumination was performed using a halogen lamp (250 W). The temperature was controlled with a helium cryostat (Oxford Instruments, UK). Samples were measured in darkness for TyrD<sup>+</sup> spectra and  $F_A/F_B$  baseline, and then, after 2-min illumination at 20 K, for the singly reduced  $F_A/F_B$  spectra. The  $F_A/F_B$  difference light-induced spectrum was used for quantitation after suppressing the P700<sup>+</sup> signal. Isolated PSI was used to check that charge separation was 100% efficient at 20 K by comparing the dithionite-reduced ( $F_A^-/F_B^-$ ) spectrum (two spins per P700) to the light-induced, singly reduced  $F_A/F_B$  difference spectrum

(one spin per PSI). The following EPR parameters were used: for TyrD<sup>+</sup>, modulation amplitude: 2 G; microwave power: 2  $\mu$ W; number of scans: eight. For F<sub>A</sub>/F<sub>B</sub> spectra, modulation amplitude: 10 G; microwave power: 0.8 mW; number of scans: two. These microwave powers were found to be nonsaturating at 20 K. The singly reduced (F<sub>A</sub>/F<sub>B</sub>) and TyrD<sup>+</sup> relative spin amounts were calculated by double integration of the EPR signals, with correction for differences in microwave power and modulation amplitude.

### Determining the Effects of Kinase Inhibitors by Phos-tag™ Gel SDS-PAGE

*S. elongatus* cells were pre-grown in fresh BG11 medium. When the cells were at 0.8 OD<sub>800</sub>, they were harvested and washed with nitrogen-free BG11 medium (BG11<sup>-N</sup>). The pellet was resuspended in BG11 medium containing 5 mM NH<sub>4</sub>Cl (BG11<sup>NH4</sup>) as the nitrogen source and incubated for 2 h. The culture was then separated into four samples. One sample was kept in the same BG11<sup>NH4</sup> medium to obtain a completely dephosphorylated P<sub>II</sub> protein.

A second sample was washed and transferred to BG11<sup>-N</sup> medium for two hours to obtain a fully phosphorylated P<sub>II</sub>. The other two samples (after the 2-h incubation in the presence of NH<sub>4</sub>Cl) were supplemented with a final concentration of 21  $\mu$ M staurosporine and 1.07  $\mu$ M K252a, respectively, and incubated for an additional hour. Finally, both samples were washed and transferred into fresh BG11<sup>-N</sup> medium in the presence of inhibitors and incubated for two more hours. The cells of all the samples were washed quickly with pre-chilled 50 mM Tris-HCl (pH 6.8) and harvested by centrifugation at 4°C.

The cell-free extracts were prepared as follows. The cells were resuspended in 500  $\mu$ L of 50 mM Tris-HCl (pH 6.8) with protease (1 mM caproic acid, 1 mM phenylmethylsulfonyl fluoride, 1 mM benzamide) and phosphatase inhibitors, and broken via five cycles of vortexing (1 min) in the presence of glass beads. Unbroken cells were removed by centrifugation and the supernatant was recovered. The phosphorylation state of PII was tested by loading the samples onto a normal 15% SDS-PAGE (polyacrylamide gel electrophoresis) gel with or without 50  $\mu$ M Zn-Phos-tag (Kinoshita and Kinoshita-Kikuta, 2011). The gels were washed with 10 mM EDTA for 3  $\times$  15 min, followed by a 10-min washing with Phos-tag gel running buffer. The gels were then blotted onto polyvinylidene difluoride membranes using a Trans-blot Turbo System (Bio-Rad Laboratories, Hercules, CA, USA). The PII band was revealed by immunoblotting with an anti-P<sub>II</sub> antibody (dilution 1:2500, kindly provided by Professor Karl Forchhammer) using a chemoluminescent detection system (Pierce).

### Accession Numbers

Sequence data from this article can be found in the GenBank/EMBL libraries under the following accession numbers: *spkA* (*sl11575*), AB046597; *spkB* (*slr1697*), AB046598; *spkC* (*slr0599*), AB046599; *spkD* (*sl10776*), AB046600; *spkE* (*slr1443*), AB046602; *spkF* (*slr1225*), AB046601; *spkG* (*slr0152*), BAA18552; *spkH* (*sl10005*), BAA10206; *spkI* (*sl11770*), BAA17672; *spkJ* (*slr0889*), BAA17617; *spkK* (*slr1919*), BAA17147; *spkL* (*sl10095*), BAA10646; *slr0328*, BAA10030; *sl11771*, BAA17671; *slr1860*, X75568; *sl11033*, BAA16771; *sl10602*, BAA10367; *slr0114*, BAA10651; *slr1983*, BAA18225; *sl1387*, BAA18237; *slr0946*, ALJ68053.

### Supplemental Data

**Supplemental Figure 1.** Gaussian decomposition of the 77 K fluorescence emission spectra of *S. elongatus*, the wild-type strains.

**Supplemental Figure 2.** Gaussian decomposition of the 77 K fluorescence emission spectra of *Synechocystis* strains.

**Supplemental Figure 3.** 77 K fluorescence emission spectra of the wild-type *S. elongatus* cells treated with Suc or phosphate buffer.

**Supplemental Figure 4.** Fluorescence changes induced by TMPD in the presence or absence of MV.

**Supplemental Figure 5.** State transitions in *Synechocystis* kinase and phosphatase mutants.

**Supplemental Figure 6.** Oxygen evolving activity in the presence of NaF.

**Supplemental Table.** Oligonucleotides used for the construction of the kinase and phosphatase mutants.

### ACKNOWLEDGMENTS

The authors thank Dr. A. Zorina for the gift of the *ΔspkH* mutant to Turku's laboratory and Professor Karl Forchhammer for the gift of the anti-P<sub>II</sub> antibody. This work was supported by the Agence Nationale de la Recherche's RECYFUEL project (grant ANR-16-CE05-0026), and from the European Union's Horizon 2020 research and innovation program (grant 675006, SE2B). P.C.'s salary is financed by the Agence Nationale de la Recherche's RECYFUEL project. The research was also supported by the Centre National de la Recherche Scientifique (CNRS), the Commissariat à l'Énergie Atomique (CEA) and the National Natural Science Foundation of China (grants 31700107 and 31770128). The French Infrastructure for Integrated Structural Biology (FRISBI) (grant ANR-10-INBS-05) also partially supported this research.

### AUTHOR CONTRIBUTIONS

P.C. performed all the experiments related to the characterization of state transitions and the role of *cyt b<sub>6</sub>f*, and analyzed data; J.Z. constructed all the kinase and phosphatase mutants, and realized almost all the experiments related with the role of phosphorylations and analyzed the data; P.S. designed, performed, analyzed, and supervised experiments; C.L., N.B., and Q.W. designed and supervised some experiments; D.K. conceived the project, designed and supervised almost all the experiments, and analyzed data; the article was written by D.K., P.S., and P.C.

Received December 3, 2018; revised February 25, 2019; accepted March 7, 2019; published March 8, 2019.

### REFERENCES

- Adir, N. (2008). Structure of the phycobilisome antennae in cyanobacteria and red algae. In Photosynthetic protein complexes: A structural approach, P. Fromme, ed (Hoboken: Wiley-VCH Verlag GmbH & Co. KGaA), pp. 243–274.
- Alfonso, M., Perewoska, I., Constant, S., and Kirilovsky, D. (1999). Redox control of *psbA* expression in cyanobacteria *Synechocystis* strains. *J. Photochem. Photobiol. Biol* **48**: 104–113.
- Alfonso, M., Perewoska, I., and Kirilovsky, D. (2000). Redox control of *psbA* gene expression in the cyanobacterium *Synechocystis* PCC 6803. Involvement of the cytochrome *b<sub>6</sub>f* complex. *Plant Physiol.* **122**: 505–516.
- Allen, J.F., Bennett, J., Steinback, K.E., and Arntzen, C.J. (1981). Chloroplast protein phosphorylation couples plastoquinone redox state to distribution of excitation energy between photosystems. *Nature* **291**: 25–29.



- Allen, J.F., Sanders, C.E., and Holmes, N.G. (1985). Correlation of membrane protein phosphorylation with excitation energy distribution in the cyanobacterium *Synechococcus* 6301. *FEBS Lett.* **193**: 271–275.
- Angeleri, M., Zorina, A., Aro, E.M., and Battchikova, N. (2018). Interplay of SpkG kinase and the Slr0151 protein in the phosphorylation of ferredoxin 5 in *Synechocystis* sp. strain PCC 6803. *FEBS Lett.* **592**: 411–421.
- Aoki, M., and Katoh, S. (1982). Oxidation and reduction of plastoquinone by photosynthetic and respiratory electron transport in a cyanobacterium *Synechococcus* sp. *Biochim. Biophys. Acta* **682**: 307–314.
- Aspinwall, C.L., Sarcina, M., and Mullineaux, C.W. (2004). Phycobilisome mobility in the cyanobacterium *Synechococcus* sp. PCC7942 is influenced by the trimerisation of Photosystem I. *Photosynth. Res.* **79**: 179–187.
- Bellafore, S., Barneche, F., Peltier, G., and Rochaix, J.D. (2005). State transitions and light adaptation require chloroplast thylakoid protein kinase STN7. *Nature* **433**: 892–895.
- Bennoun, P. (1982). Evidence for a respiratory chain in the chloroplast. *Proc. Natl. Acad. Sci. USA* **79**: 4352–4356.
- Biggins, J., and Bruce, D. (1989). Regulation of excitation energy transfer in organisms containing phycobilins. *Photosynth. Res.* **20**: 1–34.
- Biggins, J., Tanguay, N.A., and Frank, H.A. (1989). Electron transfer reactions in photosystem I following vitamin K1 depletion by ultraviolet irradiation. *FEBS Lett.* **250**: 271–274.
- Bonaventura, C., and Myers, J. (1969). Fluorescence and oxygen evolution from *Chlorella pyrenoidosa*. *Biochim. Biophys. Acta* **189**: 366–383.
- Breyton, C. (2000). Conformational changes in the cytochrome b6f complex induced by inhibitor binding. *J. Biol. Chem.* **275**: 13195–13201.
- Bruce, D., and Biggins, J. (1985). Mechanism of the light state transition in photosynthesis V. 77K linear dichroism of *Anacystis nidulans* in state 1 and state 2. *Biochim. Biophys. Acta* **810**: 295–301.
- Bruce, D., and Salehian, O. (1992). Laser-induced optoacoustic calorimetry of cyanobacteria. The efficiency of primary photosynthetic processes in state 1 and state 2. *Biochim. Biophys. Acta* **1100**: 242–250.
- Bruce, D., Brimble, S., and Bryant, D.A. (1989). State transitions in a phycobilisome-less mutant of the cyanobacterium *Synechococcus* sp. PCC 7002. *Biochim. Biophys. Acta* **974**: 66–73.
- Campbell, D., Hurry, V., Clarke, A.K., Gustafsson, P., and Öquist, G. (1998). Chlorophyll fluorescence analysis of cyanobacterial photosynthesis and acclimation. *Microbiol. Mol. Biol. Rev.* **62**: 667–683.
- Chen, Z., Zhan, J., Chen, Y., Yang, M., He, C., Ge, F., and Wang, Q. (2015). Effects of phosphorylation of  $\beta$  subunits of phycocyanins on state transition in the model cyanobacterium *Synechocystis* sp. PCC 6803. *Plant Cell Physiol.* **56**: 1997–2013.
- Chukhutsina, V., Bersanini, L., Aro, E.M., and van Amerongen, H. (2015). Cyanobacterial light-harvesting phycobilisomes uncouple from photosystem I during dark-to-light transitions. *Sci. Rep.* **5**: 14193.
- Delphin, E., Duval, J.C., and Kirilovsky, D. (1995). Comparison of state 1 state 2 transitions in the green alga *Chlamydomonas reinhardtii* and in the red alga *Rhodella violacea*: Effect of kinase and phosphatase inhibitors. *Biochimica et Biophysica Acta—Bioenergetics* **1232**: 91–95.
- Delphin, E., Duval, J.C., Etienne, A.L., and Kirilovsky, D. (1996). State transitions or delta pH-dependent quenching of photosystem II fluorescence in red algae. *Biochemistry* **35**: 9435–9445.
- Depège, N., Bellafore, S., and Rochaix, J.D. (2003). Role of chloroplast protein kinase Stt7 in LHCII phosphorylation and state transition in *Chlamydomonas*. *Science* **299**: 1572–1575.
- Dong, C., and Zhao, J. (2008). ApcD is required for state transition but not involved in blue-light induced quenching in the cyanobacterium *Anabaena* sp. PCC7120. *Chin. Sci. Bull.* **53**: 3422–3424.
- Dong, C., Tang, A., Zhao, J., Mullineaux, C.W., Shen, G., and Bryant, D.A. (2009). ApcD is necessary for efficient energy transfer from phycobilisomes to photosystem I and helps to prevent photoinhibition in the cyanobacterium *Synechococcus* sp. PCC 7002. *Biochim. Biophys. Acta* **1787**: 1122–1128.
- Draber, W., Trebst, A., and Harth, E. (1970). On a new inhibitor of photosynthetic electron-transport in isolated chloroplasts. *Z. Naturforsch. B* **25**: 1157–1159.
- El Bissati, K., and Kirilovsky, D. (2001). Regulation of *psbA* and *psaE* expression by light quality in *Synechocystis* species PCC 6803. A redox control mechanism. *Plant Physiol.* **125**: 1988–2000.
- El Bissati, K., Delphin, E., Murata, N., Etienne, A., and Kirilovsky, D. (2000). Photosystem II fluorescence quenching in the cyanobacterium *Synechocystis* PCC 6803: Involvement of two different mechanisms. *Biochim. Biophys. Acta* **1457**: 229–242.
- Emlyn-Jones, D., Ashby, M.K., and Mullineaux, C.W. (1999). A gene required for the regulation of photosynthetic light harvesting in the cyanobacterium *Synechocystis* 6803. *Mol. Microbiol.* **33**: 1050–1058.
- Federman, S., Malkin, S., and Scherz, A. (2000). Excitation energy transfer in aggregates of Photosystem I and Photosystem II of the cyanobacterium *Synechocystis* sp. PCC 6803: Can assembly of the pigment-protein complexes control the extent of spillover? *Photosynth. Res.* **64**: 199–207.
- Fernandez, P., Saint-Joanis, B., Barilone, N., Jackson, M., Gicquel, B., Cole, S.T., and Alzari, P.M. (2006). The Ser/Thr protein kinase PknB is essential for sustaining mycobacterial growth. *J. Bacteriol.* **188**: 7778–7784.
- Finazzi, G., Zito, F., Barbagallo, R.P., and Wollman, F.A. (2001). Contrasted effects of inhibitors of cytochrome b6f complex on state transitions in *Chlamydomonas reinhardtii*: The role of  $Q_o$  site occupancy in LHCII kinase activation. *J. Biol. Chem.* **276**: 9770–9774.
- Fischer, B.B., Eggen, R.I., Trebst, A., and Krieger-Liszskay, A. (2006). The glutathione peroxidase homologous gene *Gpxh* in *Chlamydomonas reinhardtii* is upregulated by singlet oxygen produced in photosystem II. *Planta* **223**: 583–590.
- Folea, I.M., Zhang, P., Aro, E.M., and Boekema, E.J. (2008). Domain organization of photosystem II in membranes of the cyanobacterium *Synechocystis* PCC6803 investigated by electron microscopy. *FEBS Lett.* **582**: 1749–1754.
- Forchhammer, K., and Tandeau de Marsac, N. (1995a). Functional analysis of the phosphoprotein  $P_{II}$  (*glnB* gene product) in the cyanobacterium *Synechococcus* sp. strain PCC 7942. *J. Bacteriol.* **177**: 2033–2040.
- Forchhammer, K., and Tandeau de Marsac, N. (1995b). Phosphorylation of the  $P_{II}$  protein (*glnB* gene product) in the cyanobacterium *Synechococcus* sp. strain PCC 7942: Analysis of in vitro kinase activity. *J. Bacteriol.* **177**: 5812–5817.
- Fufezan, C., Drepper, F., Juhnke, H.D., Lancaster, C.R.D., Un, S., Rutherford, A.W., and Krieger-Liszskay, A. (2005). Herbicide-induced changes in charge recombination and redox potential of  $Q_A$  in the T4 mutant of *Blastochloris viridis*. *Biochemistry* **44**: 5931–5939.
- Galkin, A.N., Mikheeva, L.E., and Shestakov, S.V. (2003). Insertionnaia inaktivatsiia genov, kodiruiushchikh serin/treoninovykh proteinkinazy eukarioticheskogo tipa u tsianobakterii *Synechocystis* sp. PCC 6803 [Insertional inactivation of genes encoding eukaryotic type serine/threonine protein kinases in cyanobacterium *Synechocystis* sp. PCC 6803]. *Mikrobiologiya* **72**: 64–69.

- Glazer, A.N.** (1984). Phycobilisome, a macromolecular complex optimized for light energy transfer. *Biochim. Biophys. Acta* **768**: 29–51.
- Guskov, A., Kern, J., Gabdulkhakov, A., Broser, M., Zouni, A., and Saenger, W.** (2009). Cyanobacterial photosystem II at 2.9-Å resolution and the role of quinones, lipids, channels and chloride. *Nat. Struct. Mol. Biol.* **16**: 334–342.
- Herdman, M., Delaney, S.F., and Carr, N.G.** (1973). A new medium for the isolation and growth of auxotrophic mutants of the blue-green alga *Anacystis nidulans*. *J. Gen. Microbiol.* **79**: 233–237.
- Hiyama, T., and Ke, B.** (1972). Difference spectra and extinction coefficients of P 700. *Biochim. Biophys. Acta* **267**: 160–171.
- Huang, C., Yuan, X., Zhao, J., and Bryant, D.A.** (2003). Kinetic analyses of state transitions of the cyanobacterium *Synechococcus* sp. PCC 7002 and its mutant strains impaired in electron transport. *Biochim. Biophys. Acta* **1607**: 121–130.
- Huang, J.Y., Chiu, Y.F., Ortega, J.M., Wang, H.T., Tseng, T.S., Ke, S.C., Roncel, M., and Chu, H.A.** (2016). Mutations of cytochrome  $b_{559}$  and PsbJ on and near the  $Q_C$  site in Photosystem II influence the regulation of short-term light response and photosynthetic growth of the cyanobacterium *Synechocystis* sp. PCC 6803. *Biochemistry* **55**: 2214–2226.
- Joshua, S., and Mullineaux, C.W.** (2004). Phycobilisome diffusion is required for light-state transitions in cyanobacteria. *Plant Physiol.* **135**: 2112–2119.
- Kamei, A., Yuasa, T., Orikawa, K., Geng, X.X., and Ikeuchi, M.** (2001). A eukaryotic-type protein kinase, SpkA, is required for normal motility of the unicellular cyanobacterium *Synechocystis* sp. strain PCC 6803. *J. Bacteriol.* **183**: 1505–1510.
- Kaňa, R.** (2013). Mobility of photosynthetic proteins. *Photosynth. Res.* **116**: 465–479.
- Kaňa, R., Prášil, O., Komárek, O., Papageorgiou, G.C., and Govindjee, R.** (2009). Spectral characteristic of fluorescence induction in a model cyanobacterium, *Synechococcus* sp. (PCC 7942). *Biochim. Biophys. Acta* **1787**: 1170–1178.
- Kinoshita, E., and Kinoshita-Kikuta, E.** (2011). Improved Phos-tag SDS-PAGE under neutral pH conditions for advanced protein phosphorylation profiling. *Proteomics* **11**: 319–323.
- Kirilovsky, D., Rutherford, A.W., and Etienne, A.L.** (1994). Influence of DCMU and ferricyanide on photodamage in photosystem II. *Biochemistry* **33**: 3087–3095.
- Kondo, K., Mullineaux, C.W., and Ikeuchi, M.** (2009). Distinct roles of CpcG1-phycobilisome and CpcG2-phycobilisome in state transitions in a cyanobacterium *Synechocystis* sp. PCC 6803. *Photosynth. Res.* **99**: 217–225.
- Kowalczyk, N., Rappaport, F., Boyen, C., Wollman, F.A., Collén, J., and Joliot, P.** (2013). Photosynthesis in *Chondrus crispus*: The contribution of energy spill-over in the regulation of excitonic flux. *Biochim. Biophys. Acta* **1827**: 834–842.
- Kruip, J., Bald, D., Boekema, E., and Rögner, M.** (1994). Evidence for the existence of trimeric and monomeric Photosystem I complexes in thylakoid membranes from cyanobacteria. *Photosynth. Res.* **40**: 279–286.
- Krupnik, T., Kotabová, E., van Bezouwen, L.S., Mazur, R., Garstka, M., Nixon, P.J., Barber, J., Kaňa, R., Boekema, E.J., and Kargul, J.** (2013). A reaction center-dependent photoprotection mechanism in a highly robust photosystem II from an extremophilic red alga, *Cyanidioschyzon merolae*. *J. Biol. Chem.* **288**: 23529–23542.
- Kyle, D.J., Ohad, I., and Arntzen, C.J.** (1984). Membrane protein damage and repair: Selective loss of a quinone-protein function in chloroplast membranes. *Proc. Natl. Acad. Sci. USA* **81**: 4070–4074.
- Laurent, S., Jang, J., Janicki, A., Zhang, C.C., and Bédu, S.** (2008). Inactivation of spkD, encoding a Ser/Thr kinase, affects the pool of the TCA cycle metabolites in *Synechocystis* sp. strain PCC 6803. *Microbiology* **154**: 2161–2167.
- Ley, A.C., and Butler, W.L.** (1980). Energy distribution in the photochemical apparatus of *Porphyridium cruentum* in state I and state II. *Biochim. Biophys. Acta* **592**: 349–363.
- Li, D., Xie, J., Zhao, J., Xia, A., Li, D., and Gong, Y.** (2004). Light-induced excitation energy redistribution in *Spirulina platensis* cells: “Spillover” or “mobile PBSs”? *Biochim. Biophys. Acta* **1608**: 114–121.
- Li, H., Li, D., Yang, S., Xie, J., and Zhao, J.** (2006). The state transition mechanism—Simply depending on light-on and -off in *Spirulina platensis*. *Biochim. Biophys. Acta* **1757**: 1512–1519.
- Liang, C., Zhang, X., Chi, X., Guan, X., Li, Y., Qin, S., and Shao, H.B.** (2011). Serine/threonine protein kinase SpkG is a candidate for high salt resistance in the unicellular cyanobacterium *Synechocystis* sp. PCC 6803. *PLoS One* **6**: e18718.
- MacColl, R.** (1998). Cyanobacterial phycobilisomes. *J. Struct. Biol.* **124**: 311–334.
- Mao, H.B., Li, G.F., Ruan, X., Wu, Q.Y., Gong, Y.D., Zhang, X.F., and Zhao, N.M.** (2002). The redox state of plastoquinone pool regulates state transitions via cytochrome b6f complex in *Synechocystis* sp. PCC 6803. *FEBS Lett.* **519**: 82–86.
- Mao, L., Wang, Y., and Hu, X.** (2003). II-II stacking interactions in the peridinin-chlorophyll-protein of *Amphidinium carterae*. *J. Phys. Chem. B* **107**: 3963–3971.
- Mata-Cabana, A., García-Domínguez, M., Florencio, F.J., and Lindahl, M.** (2012). Thiol-based redox modulation of a cyanobacterial eukaryotic-type serine/threonine kinase required for oxidative stress tolerance. *Antioxid. Redox Signal.* **17**: 521–533.
- McCartney, B., Howell, L.D., Kennelly, P.J., and Potts, M.** (1997). Protein tyrosine phosphorylation in the cyanobacterium *Anabaena* sp. strain PCC 7120. *J. Bacteriol.* **179**: 2314–2318.
- McConnell, M.D., Koop, R., Vasil'ev, S., and Bruce, D.** (2002). Regulation of the distribution of chlorophyll and phycobilin-absorbed excitation energy in cyanobacteria. A structure-based model for the light state transition. *Plant Physiol.* **130**: 1201–1212.
- Minagawa, J.** (2011). State transitions—The molecular remodeling of photosynthetic supercomplexes that controls energy flow in the chloroplast. *Biochim. Biophys. Acta* **1807**: 897–905.
- Misumi, M., Katoh, H., Tomo, T., and Sonoike, K.** (2016). Relationship between photochemical quenching and non-photochemical quenching in six species of cyanobacteria reveals species difference in redox state and species commonality in energy dissipation. *Plant Cell Physiol.* **57**: 1510–1517.
- Mullineaux, C.W.** (2014). Co-existence of photosynthetic and respiratory activities in cyanobacterial thylakoid membranes. *Biochim. Biophys. Acta* **1837**: 503–511.
- Mullineaux, C.W., and Allen, J.F.** (1986). The state 2 transition in the cyanobacterium *Synechococcus* 6301 can be driven by respiratory electron flow into the plastoquinone pool. *FEBS Lett.* **205**: 155–160.
- Mullineaux, C.W., and Allen, J.F.** (1990). State 1 State 2 transitions in the cyanobacterium *Synechococcus* 6301 are controlled by the redox state of electron carriers between Photosystems I and II. *Photosynth. Res.* **23**: 297–311.
- Mullineaux, C.W., Griebenow, S., and Braslavsky, S.E.** (1991). Photosynthetic energy storage in cyanobacterial cells adapted to light-states 1 and 2. A laser-induced optoacoustic study. *Biochim. Biophys. Acta* **1060**: 315–318.
- Mullineaux, C.W., Tobin, M.J., and Jones, G.R.** (1997). Mobility of photosynthetic complexes in thylakoid membranes. *Nature* **390**: 421–424.
- Murata, N.** (1969). Control of excitation transfer in photosynthesis. I. Light-induced change of chlorophyll a fluorescence in *Porphyridium cruentum*. *Biochim. Biophys. Acta* **172**: 242–251.

- Nakano, H., and Omura, S.** (2009). Chemical biology of natural indolocarbazole products: 30 years since the discovery of staurosporine. *J. Antibiot. (Tokyo)* **62**: 17–26.
- Nanba, M., and Katoh, S.** (1985). Restoration by tetramethyl-*p*-phenylenediamine of photosynthesis in dibromothymoquinone-inhibited cells of the cyanobacterium *Synechococcus* sp. *Biochim. Biophys. Acta* **809**: 74–80.
- Olive, J., M'Bina, I., Vernotte, C., Astier, C., and Wollman, F.A.** (1986). Randomization of the Ef particles in thylakoid membranes of *Synechocystis* 6714 upon transition from state-I to state-II. *FEBS Lett.* **208**: 308–312.
- Olive, J., Ajlani, G., Astier, C., Recouvreur, M., and Vernotte, C.** (1997). Ultrastructure and light adaptation of phycobilisome mutants of *Synechocystis* PCC 6803. *Biochim. Biophys. Acta* **1319**: 275–282.
- Panichkin, V.B., Arakawa-Kobayashi, S., Kanaseki, T., Suzuki, I., Los, D.A., Shestakov, S.V., and Murata, N.** (2006). Serine/threonine protein kinase SpkA in *Synechocystis* sp. strain PCC 6803 is a regulator of expression of three putative *pilA* operons, formation of thick pili, and cell motility. *J. Bacteriol.* **188**: 7696–7699.
- Papageorgiou G.C., Govindjee, R., Mimuro, M., Stamatakis, K., Alygizaki-Zorba, A., and Murata, N.** (1999). Light-induced and osmotically-induced changes in chlorophyll a fluorescence in two *Synechocystis* sp. PCC 6803 strains that differ in membrane lipid unsaturation. *Photosynth. Res.* **59**: 125–136.
- Preston, C., and Critchley, C.** (1988). Interaction of electron acceptors with thylakoids from halophytic and non-halophytic species. *Photosynth. Res.* **16**: 187–202.
- Ranjbar Choubeh, R., Wientjes, E., Struik, P.C., Kirilovsky, D., and van Amerongen, H.** (2018). State transitions in the cyanobacterium *Synechococcus elongatus* 7942 involve reversible quenching of the photosystem II core. *Biochim Biophys Acta Bioenerg* **1859**: 1059–1066.
- Roberts, A.G., and Kramer, D.M.** (2001). Inhibitor “double occupancy” in the  $Q_o$  pocket of the chloroplast cytochrome  $b_6f$  complex. *Biochemistry* **40**: 13407–13412.
- Schluchter, W.M., Shen, G., Zhao, J., and Bryant, D.A.** (1996). Characterization of *psal* and *psaL* mutants of *Synechococcus* sp. strain PCC 7002: A new model for state transitions in cyanobacteria. *Photochem. Photobiol.* **64**: 53–66.
- Scott, M., McCollum, C., Vasil'ev, S., Crozier, C., Espie, G.S., Krol, M., Huner, N.P., and Bruce, D.** (2006). Mechanism of the down regulation of photosynthesis by blue light in the Cyanobacterium *Synechocystis* sp. PCC 6803. *Biochemistry* **45**: 8952–8958.
- Siefermann-Harms, D** (1988). Application of chlorophyll fluorescence. In *Fluorescence properties of isolated chlorophyll-protein complexes.*, HK Lichtenthaler, ed (Dordrecht: Kluwer Academic Publisher), pp. 45–54.
- Spät, P., Maček, B., and Forchhammer, K.** (2015). Phosphoproteome of the cyanobacterium *Synechocystis* sp. PCC 6803 and its dynamics during nitrogen starvation. *Front. Microbiol.* **6**: 248.
- Srivastava, A., Strasser, R.J., and Govindjee, R.** (1995). Polyphasic rise of chlorophyll a fluorescence in herbicide-resistant D1 mutants of *Chlamydomonas reinhardtii*. *Photosynth. Res.* **43**: 131–141.
- Umena, Y., Kawakami, K., Shen, J.R., and Kamiya, N.** (2011). Crystal structure of oxygen-evolving photosystem II at a resolution of 1.9 Å. *Nature* **473**: 55–60.
- Van Dorssen, R.J, Breton, J, Plijter, J.J, Satoh, K, Van Gorkom, H.J, and Amesz, J.** (1987). Spectroscopic properties of the reaction center and of the 47 kDa chlorophyll protein of photosystem II. *Biochim Biophys Acta* **893**: 267–274.
- Vener, A.V., Van Kan, P.J., Gal, A., Andersson, B., and Ohad, I.** (1995). Activation/deactivation cycle of redox-controlled thylakoid protein phosphorylation. Role of plastoquinol bound to the reduced cytochrome *bf* complex. *J. Biol. Chem.* **270**: 25225–25232.
- Vener, A.V., van Kan, P.J., Rich, P.R., Ohad, I., and Andersson, B.** (1997). Plastoquinol at the quinol oxidation site of reduced cytochrome *bf* mediates signal transduction between light and protein phosphorylation: Thylakoid protein kinase deactivation by a single-turnover flash. *Proc. Natl. Acad. Sci. USA* **94**: 1585–1590.
- Vernotte, C., Picaud, M., Kirilovsky, D., Olive, J., Ajlani, G., and Astier, C.** (1992). Changes in the photosynthetic apparatus in the cyanobacterium *Synechocystis* sp. PCC 6714 following light-to-dark and dark-to-light transitions. *Photosynth. Res.* **32**: 45–57.
- Vladkova, R.** (2016). Chlorophyll a is the crucial redox sensor and transmembrane signal transmitter in the cytochrome  $b_6f$  complex. Components and mechanisms of state transitions from the hydrophobic mismatch viewpoint. *J. Biomol. Struct. Dyn.* **34**: 824–854.
- Wollman, F.A.** (2001). State transitions reveal the dynamics and flexibility of the photosynthetic apparatus. *EMBO J.* **20**: 3623–3630.
- Wollman, F.A., and Lemaire, C.** (1988). Studies on kinase-controlled state transitions in Photosystem II and  $b_6f$  mutants from *Chlamydomonas reinhardtii* which lack quinone-binding proteins. *Biochim. Biophys. Acta* **933**: 85–94.
- Yang, M.K., Qiao, Z.X., Zhang, W.Y., Xiong, Q., Zhang, J., Li, T., Ge, F., and Zhao, J.D.** (2013). Global phosphoproteomic analysis reveals diverse functions of serine/threonine/tyrosine phosphorylation in the model cyanobacterium *Synechococcus* sp. strain PCC 7002. *J. Proteome Res.* **12**: 1909–1923.
- Zhang, Z., Huang, L., Shulmeister, V.M., Chi, Y.I., Kim, K.K., Hung, L.W., Crofts, A.R., Berry, E.A., and Kim, S.H.** (1998). Electron transfer by domain movement in cytochrome  $bc_1$ . *Nature* **392**: 677–684.
- Zito, F., Finazzi, G., Delosme, R., Nitschke, W., Picot, D., and Wollman, F.A.** (1999). The  $Q_o$  site of cytochrome  $b_6f$  complexes controls the activation of the LHClI kinase. *EMBO J.* **18**: 2961–2969.
- Zorina, A.A.** (2013). Eukaryotic protein kinases in cyanobacteria. *Russ. J. Plant Physiol.* **60**: 589–596.
- Zorina, A., Stepanchenko, N., Novikova, G.V., Sinetova, M., Panichkin, V.B., Moshkov, I.E., Zinchenko, V.V., Shestakov, S.V., Suzuki, I., Murata, N., and Los, D.A.** (2011). Eukaryotic-like Ser/Thr protein kinases SpkC/F/K are involved in phosphorylation of GroES in the cyanobacterium *synechocystis*. *DNA Res.* **18**: 137–151.
- Zorina, A.A., Bedbenov, V.S., Novikova, G.V., Panichkin, V.B., and Los, D.A.** (2014). [Involvement of serine/threonine protein kinases in cold stress response in the cyanobacterium *Synechocystis* sp. PCC 6803: Functional characterization of a protein kinase SpkE]. *Mol. Biol. (Mosk.)* **48**: 452–462.